國立交通大學

電信工程研究所

碩士論文

無線網路編碼系統中的訊號偵測

Signal Detection in a Wireless Network-Coded System

研究生：鄭　瑩

指導教授：蘇育德　教授

中華民國九十九年十一月

無線網路編碼系統中的訊號偵測
Signal Detection in a Wirework-Coded System

研 究 生：鄭　瑩　　Student：Ying Cheng

指導教授：蘇育德　　Advisor：Yu-Ted Su

國 立 交 通 大 學

電 信 工 程 研 究 所

碩 士 論 文

A Thesis

Submitted to Department of Communication Engineering

College of Electrical and Computer Engineering

National Chiao Tung University

in partial Fulfillment of the Requirements

for the Degree of

Master

in

Communication Engineering

Nov 2010

Hsinchu, Taiwan, Republic of China

中華民國九十九年十一月

無線網路編碼系統中的訊號偵測

學生：鄭　瑩　　指導教授：蘇育德　博士

國立交通大學電信工程學系碩士班

摘　　要

近來實體層（無線）網路編碼因為可提高了吞吐量而引起不少研究者的興趣。在無線傳輸環境中，接收器收到的訊號常常是不同來源的信號和雜訊的疊加。相較於傳統接收器試圖估測其中個別的信號，作為有網路編碼網路的中繼接收機，則只需要估計兩個同時到達信號的和或差。

本篇論文主要目的是在研究當中繼接收機所收到的無線信號為二元相移鍵調變或二元頻率鍵移調變時的訊號檢測。我們首先在時間同步的情況下推導出訊號檢測的架構及其錯誤率表現。接著討論在固定和隨機時間偏移時如何檢測兩個信號的編碼和。我們的分析有助於瞭解實體層網路編碼在什麼樣的條件下方可提升系統吞吐量。

Signal Detection in A Wireless Network-Coded System

Student：Ying Cheng　　Advisor：Yu T. Su

Department of Communication Engineering

National Chiao Tung University

ABSTRACT

Physical layer network coding (PNC) has drew much attention due to its potential of bringing about significant throughput enhancement. In a wireless environment, a received signal is often resulted from the superposition of the signals and noises from various sources. Instead of detecting one or more signal, the responsibility of a relay receiver in a wireless network-coded system is to estimate the algebraic sum of the (two) incoming binary waveforms.

The aim of this thesis is to solve the above signal detection problem when binary frequency-shift-keying (BFSK) modulation is used. We first derive the detector structure in a network with perfect timing synchronization and analyze the resulting bit error rate performance. We then consider the scenarios when either a fixed or a random timing offset is present. The performance analysis shows that the network throughput can indeed be improved through PNC if proper conditions are met.

誌　　謝

這份論文的完成，首先感謝我的指導老師 蘇育德博士一路以來的包容和提攜。在學術方面指引我學習的方法和整體的概念，更著重口條訓練以及個人儀態等全方面學習。此外對於生活體驗的鼓勵與分享，令我受益匪淺。

感謝引領我進入論文研究領域的人仰學長，博學多聞又很有耐心，除了專業知識的指導，平時遇到挫折時也給我鼓舞和建議。另外由衷的感謝一起努力的同學和學弟妹們，相處時分享的喜怒哀樂是這段時光的精神寄託。

最後感謝我的家人，默默給我的支持、關心和照顧是我一路以來的力量泉源。謹以此篇論文代表我最深的敬意。

Contents

List of Figures

List of Tables

Signal Detection in A Wireless Network-Coded System

Student : Ying Cheng Advisor : Yu T. Su

Department of Communications Engineering

National Chiao Tung University

Abstract

Physical layer network coding (PNC) has drew much attention due to its potential of bringing about significant throughput enhancement. In a wireless environment, a received signal is often resulted from the superposition of the signals and noises from various sources. Instead of detecting individual signals, a relay in a wireless PNC-coded relay network has to estimate the encoded output only. For example, if a relay receives two incoming binary waveforms, it has to estimate the algebraic sum of the (two) binary symbols.

The aim of this thesis is to solve the above signal detection and estimation problem when noncoherent binary frequency-shift-keying (BFSK) modulation is used to avoid the need of phase pre-compensations at the source nodes. We first derive the optimal and suboptimal detector structures in a network with perfect timing synchronization and analyze the resulting bit error rate performance. We then extend our investigation to the scenarios when either a fixed or a random timing timing offset is present. The performance analysis shows that the network throughput can indeed be improved through PNC if proper conditions are met.

Chapter 1

Introduction

Recently, physical-layer Network Coding (PNC) has been appealing lots of attention within wireless communication society due to the significant improvement of throughput. [1]-[4], for example, show the noticeable throughput improvement under various wireless networks. Specifically, a MAC layer protocol (COPE) based on the concept of PNC is proposed in [2] and it is shown that COPE can be applied in an Ad Hoc or Mesh access network. A regular 1 dimension (1D) linear network system is considered in [3] with 100% throughput improvement compared with traditional transmission scheme. Moreover, it is also shown that PNC can achieve the upper-bound capacity. In [4], the authors propose scheduling algorithms for PNC in 2 dimension(2D) regular networks and, in this case, 200% throughput improvement is achieved.

In this thesis, we consider a wireless network composed of two source nodes and a relay node, as shown in Fig. 1.1. It is assumed that the two source nodes want to exchange the information and is accomplished via the relay node. This situation occurs when two source nodes are apart from. Because of the implement issue, a half-duplex system is considered (no transmission and reception occurs simultaneously).

In a traditional system, the relay node receives the signal sent from one source, and send the detected result to the other node at the next time slot. Hence, to complete a exchange for two source nodes, four time slot is required in this system, as illustrated in Fig. 1.2. The throughput in the system is $\frac{1}{4}$ symbol per user per time slot (Sym/U/TS).

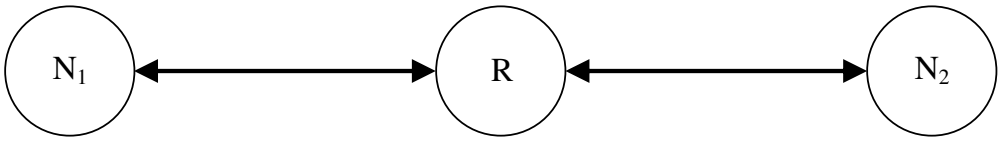

Figure 1.1: Three nodes system which includes one relay node and two end nodes.

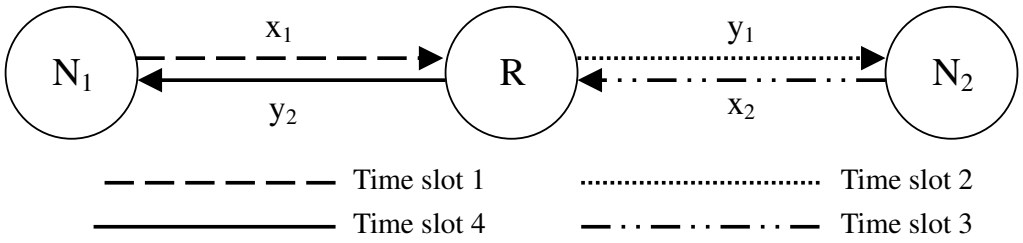

Figure 1.2: Traditional system to exchange data by the relay node.

To improve the throughput, network coding scheme can be applied at relay. As illustrated in Fig. 1.3, two time slots are devoted to the transmission from source nodes to relay. Then, the relay encodes the received signals and broadcast it. In this scheme (called three-phase transmission communication(TPTC)), the throughput of the network is $\frac{1}{3}$(Sym/U/TS).

Notice that the property of wireless environment, broadcast, is used in the third time slot in TPTC. In fact, this property can also be used to improve the throughput by

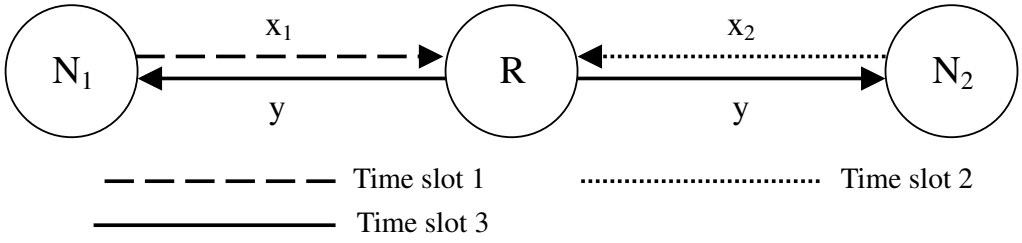

Figure 1.3: TPTC system to exchange data by the relay node.

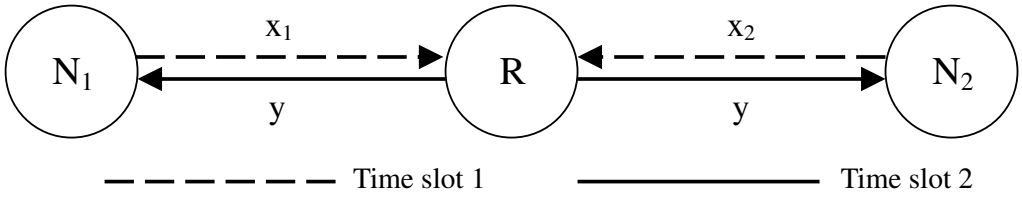

Figure 1.4: PNC system to exchange data by the relay node.

allowing the transmissions of two source nodes at the same time slot (Fig. 1.4). Although the two source nodes interfere with each other, it is clear that the throughput can be enhanced if the relay node can detect the signals without error. Hence, it is important point to study the optimal detection at relay node such that the enhancement can be achieved.

In [5], the optimal mapping function at the relay node that minimizes the bit-error rate (BER) over Rayleigh fading channels and the associated performance analysis were proposed. We point out that the detector considered in this paper is not a maximum likelihood (ML) detector and it can be shown that the former detector can be obtained from ML detector with some approximation. The symbol error rate performance with ML detector and BPSK/QPSK modulation is studied in [6] for the system with PNC over AWGN channels. Different from the previous mentioned work, [7] investigates a relay system with multiple antennas at the source nodes.

As can be seen, synchronization among each node is a key requirement to provide the improvement. [8] shows that the performance loss with BPSK modulation in the presence of timing or phase error (but not both) is about 3dB. However, power control is required such that the received signals from source nodes have the same amplitude. In practical system, it is hard to have exact power control and the performance loss is larger. In order to avoid the synchronization requirement, non-coherent detection is considered in [9] and [10]. [10] shows that the average expected throughput performance

using BFSK has similar behavior as BPSK, and [9] describes a different detection model of BFSK according to various channel information.

In this thesis, we consider the noncoherent detection and the associated performance analysis of PNC under BFSK in Rayleigh fading channel. Different from the work [9], we focus on the detection without any channel information and two suboptimal detectors with negligible performance loss are proposed. The associated performance is also provided. Moreover, we also consider the noncoherent detection with timing misalignment.

The reset of this thesis is organized as follows. In section II, the system model with and without timing error is provided and the optimal and suboptimal detectors are derived based on the system model. Due to the negligible performance loss, performance analysis based on the suboptimal detectors are provided in section IV and we justify our analysis through simulation in the following section. Some discussions of the performance with and without timing misalignment are included in the same section. Finally, we draw some conclusions to end up this thesis.

Chapter 2

System model

In this section, we describe the PNC system models and notations considered in this thesis. For physical-layer network coding (PNC) scheme in a three terminal network, each of the end nodes $N_i, i = 1, 2$ transmits the information $b_i \in \{0, 1\}$ simultaneously to the relay over a flat-fading channel, as shown in Fig. 2.1. Let h_i represent the complex value channel coefficient from node N_i to the relay. The coefficient can be represented as $h_i = \alpha_i e^{\theta_i}$, where α_i is the received amplitude and θ_i is the phase shift due to the fading, the transmitter's continuous-phase constraint, and the offset between the transmitter's oscillator and receiver's oscillator.

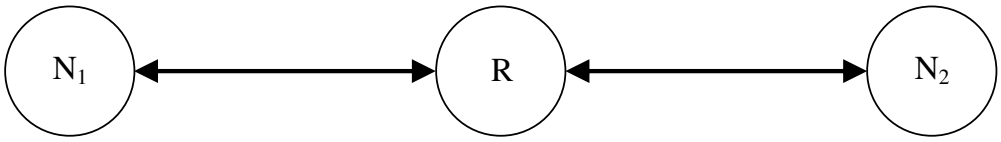

Figure 2.1: Information exchange between N_1 and N_2 among R.

2.1 Case 1: perfect timing synchronization

Suppose the timing is synchronized such that the signals from node N_1 and N_2 are arrived at the relay at the same time. Then the received waveform at the relay is $y_p(t)$ which consists of these components : the combination of signals from two source and

the noise term. The received waveform can be represented as

$$y_p(t) = h_1 x_{p1}(t) + h_2 x_{p2}(t) + n_p(t) \tag{2.1}$$

where $x_{pi}(t) = \{e^{j2\pi(f_0 + b_i \triangle f)t}\}$ with $b_i \in \{0, 1\}$, channel spacing $\triangle\ f = \frac{1}{T_s}$, and subcarrier f_0. $n_p(t)$ is zero mean additive white Gaussian noise (AWGN) with two-sided power spectral density $\frac{N_0}{2}\ W/H_z$ and the channel coefficient h_i is modeled as a complex Gaussian random variable with zero mean and variance P_{si}. Do notice that the transmission power factor of N_i is incorporated into the variance of h_i.

The equivalent baseband model of (2.1) is

$$\mathbf{y} = h_1 \mathbf{x}_1 + h_2 \mathbf{x}_2 + \mathbf{n} \tag{2.2}$$

where

$$\mathbf{y} = \begin{bmatrix} y_1 \\ y_2 \end{bmatrix}, \mathbf{n} = \begin{bmatrix} n_1 \\ n_2 \end{bmatrix},$$

$\mathbf{y}$ is the equivalent received signal vector at relay node and $\mathbf{n}$ is a zero mean circularly symmetric complex Gaussian noise with covariance matrix $\sigma_0^2 \mathbf{I}_2$, where $\mathbf{I}_2$ is the 2-by-2 identity matrix and $\sigma_0^2 = N_0$. The transmission signal vector $\mathbf{x}_i$ is represented by

$$\mathbf{x}_i = [(1 - b_i) \quad b_i]^T\ , \quad i = 1, 2 \tag{2.3}$$

The possible combinations of transmitted bits are represented by four events:

event	$\mathbb{E}_1$	$\mathbb{E}_2$	$\mathbb{E}_3$	$\mathbb{E}_4$
b_1	0	1	0	1
b_2	0	1	1	0

Specifically, given the event $\mathbb{E}_i$, the signal received by the relay is $\mathbf{y} = \mathbf{m}_i + \mathbf{n}$,where

$$\mathbf{m}_1 = [(h_1 + h_2) \quad 0]^T \qquad \mathbf{m}_2 = [0 \quad (h_1 + h_2)]^T$$
$$\mathbf{m}_3 = [h_1 \quad h_2]^T \qquad \mathbf{m}_4 = [h_2 \quad h_1]^T \tag{2.4}$$

2.2 Case 2: timing alignment error

In practical, to achieve the perfect timing alignment, the relay node should estimate the timing offset of signals from N_1 and N_2, and feedback the information to source nodes perfectly. It is, however, difficult to estimate the timing offset without error and this information may be outdated due to the delay. Due to the practical consideration, we are interested in asynchronous PNC signal detection scheme and the system model should be provided. In this section, we establish the system model and the signal detection scheme is discussed later.

Under timing alignment error, suppose a timing offset $\epsilon_i T_s$ for N_1 and N_2 appears when the relay node receives signals from end nodes, where ϵ_i is a random variable and T_s is the symbol duration time. Before deriving the equivalent baseband system model, we define a duration interval function.

$$P_{T_s}(t) = \begin{cases} 1, & 0 \le t < T_c \\ 0, & otherwise. \end{cases} \tag{2.5}$$

Then, the baseband signal $x_{pi}(t)$, $i = 0, 1$ is

$$x_{pi}(t) = P_{T_s}(t - \epsilon_i T_s) e^{j2\pi(f_0 + b_i \triangle f)t}$$

and the received signal at relay is the same as (2.1). Again, do notice that the power factor is incorporated into the variance of channel coefficient.

In this thesis, we assume that no inter-symbol interference (ISI) appears. This assumption is rational if there is a sufficient long guard time between the two successive symbols. Based on this assumption, the match filter output for ith frequency band (Fig. 2.2) is

$$\begin{aligned} y_i &= \int_0^{T_s} y(t) e^{-j2\pi(f_0 + (i-1)\triangle f)t} dt \\ &= \int_0^{T_s} (h_1 x_{p1}(t) + h_2 x_{p2}(t)) e^{-j2\pi(f_0 + (i-1)\triangle f)t} dt + n \\ &\triangleq S_i + n \qquad i = 1, 2 \end{aligned}$$

where S_i denotes the signal part and n is the noise. Because the noise n has been discussed in the previous section, to find the equivalent baseband model, we only need to calculate S.

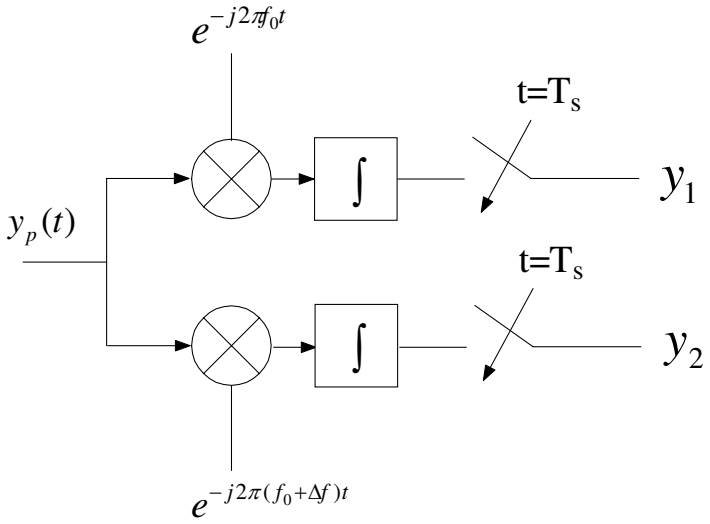

Figure 2.2: The structure of match filter bank.

Due to the symmetry of the signal part from N_1 and N_2, it is sufficient to consider the signal part from N_1 only. Suppose $\epsilon_1 > 0$, then we have

$$\begin{aligned} S_{i1} &= h_1 \int_0^{T_c} P_{T_c}(t-\epsilon_1 T_c)(t) e^{j(2\pi(b_1-i+1)\triangle f t)} dt \\ &= h_1 \int_{\epsilon_1 T_c}^{T_c} e^{j(2\pi(b_1-i+1)\triangle f t)} dt \end{aligned}$$

where S_{i1} denote the signal part consisting of the signal from N_1.

Observe that

$$\begin{aligned} \int_{\epsilon_1 T_c}^{T_c} e^{j(2\pi(b_1-i+1)\triangle f t)} dt &= \frac{e^{j\pi(b_1-i+1)\triangle f(1+\epsilon_1)T_c}}{\pi(b_1-i+1)\ \triangle\ f} \frac{1}{2j} \left(e^{j\pi(b_1-i+1)\triangle f(1-\epsilon_1)T_c} - e^{-j\pi(b_1-i+1)\triangle f(1-\epsilon_1)T_c}\right) \\ &= e^{j\pi(b_1-i+1)\triangle f(1+\epsilon_1)T_c} \frac{\sin\left(\pi(b_1-i+1)\ \triangle\ f(1-\epsilon_1)T_c\right)}{\pi(b_1-i+1)\ \triangle\ f} \\ &= e^{j\pi(b_1-i+1)\triangle f(1+\epsilon_1)T_c} (1-\epsilon_1)T_c \operatorname{sinc}\left((b_1-i+1)\ \triangle\ f(1-\epsilon_1)T_c\right) \end{aligned}$$

where

$$\operatorname{sinc}(x) \triangleq \frac{\sin(\pi x)}{\pi x}$$

Hence, the signal part S_i is

$$S_{i1} = h_1 e^{j\pi(b_1-i+1)\triangle f(1+\epsilon_1)T_c}(1-\epsilon_1)T_c \,\mathrm{sinc}\left((b_1-i+1)\triangle f(1-\epsilon_1)T_c\right) \quad (2.6)$$

Similarly, for $\epsilon_1 < 0$, the signal part S_{i1} is

$$\begin{aligned} S_{i1} &= h_1 \int_0^{T_c} P_{T_c}(t-\epsilon_1 T_c)(t) e^{j(2\pi(b_1-i+1)\triangle ft)} dt \\ &= h_1 \int_0^{T_c+\epsilon_1 T_c} e^{j(2\pi(b_1-i+1)\triangle ft)} dt \end{aligned}$$

Again, we focus on the integral and we have

$$\begin{aligned} \int_0^{(1+\epsilon_1)T_c} e^{j(2\pi(b_1-i+1)\triangle ft)} dt &= \frac{e^{j(2\pi(b_1-i+1)\triangle f(1+\epsilon_1)T_c}-1}{j2\pi(b_1-i+1)\triangle f} \\ &= \frac{e^{j(\pi(b_1-i+1)\triangle f(1+\epsilon_1)T_c}}{\pi(b_1-i+1)\triangle f} \frac{e^{j(\pi(b_1-i+1)\triangle f(1+\epsilon_1)T_c}-e^{-j(\pi(b_1-i+1)\triangle f(1+\epsilon_1)T_c}}{2j} \\ &= \frac{e^{j(\pi(b_1-i+1)\triangle f(1+\epsilon_1)T_c}}{\pi(b_1-i+1)\triangle f} \sin((\pi(b_1-i+1)\triangle f(1+\epsilon_1)T_c) \\ &= e^{j(\pi(b_1-i+1)\triangle f(1+\epsilon_1)T_c}(1+\epsilon_1)T_c \mathrm{sinc}((b_1-i+1)\triangle f(1+\epsilon_1)T_c) \end{aligned}$$

and

$$S_{i1} = h_1 e^{j\pi(b_1-i+1)\triangle f(1+\epsilon_1)T_c}(1+\epsilon_1)T_c \,\mathrm{sinc}\left((b_1-i+1)\triangle f(1+\epsilon_1)T_c\right) \quad (2.7)$$

From (2.6) and (2.7), the signal part can be represented as

$$S_{i1} = h_1 e^{j\pi(b_1-i+1)\triangle f(1+\epsilon_1)T_c}(1-|\epsilon_1|)T_c \,\mathrm{sinc}\left((b_1-i+1)\triangle f(1-|\epsilon_1|)T_c\right) \quad (2.8)$$

To be compact, we assume $T_c = 1$ without loss of generality and transform it into the matrix representation (2.2)

$$\mathbf{y} = h_1\mathbf{x}_1 + h_2\mathbf{x}_2 + \mathbf{n} \quad (2.9)$$

and

$$\begin{aligned} \mathbf{y} &= \begin{bmatrix} y_1 \\ y_2 \end{bmatrix} \\ &= h_1(1-|\epsilon_1|) \begin{bmatrix} 1 & e^{j\pi(1+\epsilon_1)}\mathrm{sinc}(1-|\epsilon_1|) \\ e^{-j\pi(1+\epsilon_1)}\mathrm{sinc}(1-|\epsilon_1|) & 1 \end{bmatrix} \begin{bmatrix} 1-b_1 \\ b_1 \end{bmatrix} \\ &+ h_2(1-|\epsilon_2|) \begin{bmatrix} 1 & e^{j\pi(1+\epsilon_2)}\mathrm{sinc}(1-|\epsilon_2|) \\ e^{-j\pi(1+\epsilon_2)}\mathrm{sinc}(1-|\epsilon_2|) & 1 \end{bmatrix} \begin{bmatrix} 1-b_2 \\ b_2 \end{bmatrix} + \mathbf{n} \end{aligned}$$

Similar to the case 1, we have four possibilities

event	$\mathbb{E}_1$	$\mathbb{E}_2$	$\mathbb{E}_3$	$\mathbb{E}_4$
b_1	0	1	0	1
b_2	0	1	1	0

and the corresponding received signal for the four event $\mathbb{E}_i$ is

$$\mathbf{y} = \mathbf{m}_i + \mathbf{n} \tag{2.10}$$

where

$$\begin{aligned}
\mathbf{m}_1 &= h_1(1-|\epsilon_1|)\begin{bmatrix} 1 \\ e^{-j\pi(1+\epsilon_1)}\mathrm{sinc}(1-|\epsilon_1|) \end{bmatrix} + h_2(1-|\epsilon_2|)\begin{bmatrix} 1 \\ e^{-j\pi(1+\epsilon_2)}\mathrm{sinc}(1-|\epsilon_2|) \end{bmatrix} \\
\mathbf{m}_2 &= h_1(1-|\epsilon_1|)\begin{bmatrix} e^{j\pi(1+\epsilon_1)}\mathrm{sinc}(1-|\epsilon_1|) \\ 1 \end{bmatrix} + h_2(1-|\epsilon_2|)\begin{bmatrix} e^{j\pi(1+\epsilon_2)}\mathrm{sinc}(1-|\epsilon_2|) \\ 1 \end{bmatrix} \\
\mathbf{m}_3 &= h_1(1-|\epsilon_1|)\begin{bmatrix} 1 \\ e^{-j\pi(1+\epsilon_1)}\mathrm{sinc}(1-|\epsilon_1|) \end{bmatrix} + h_2(1-|\epsilon_2|)\begin{bmatrix} e^{j\pi(1+\epsilon_2)}\mathrm{sinc}(1-|\epsilon_2|) \\ 1 \end{bmatrix} \\
\mathbf{m}_4 &= h_1(1-|\epsilon_1|)\begin{bmatrix} e^{j\pi(1+\epsilon_1)}\mathrm{sinc}(1-|\epsilon_1|) \\ 1 \end{bmatrix} + h_2(1-|\epsilon_2|)\begin{bmatrix} 1 \\ e^{-j\pi(1+\epsilon_2)}\mathrm{sinc}(1-|\epsilon_2|) \end{bmatrix}
\end{aligned} \tag{2.11}$$

Chapter 3

Receiver structure over Rayleigh fading channel

For binary modulation, a natural and popular encoding scheme at relay node is the exclusive or (XOR) scheme and the encoding rule, denoted by $\bigoplus$, is

$$0 \bigoplus 0 = 0, \qquad 1 \bigoplus 1 = 0, \tag{3.1}$$

$$1 \bigoplus 0 = 1, \qquad 0 \bigoplus 1 = 1. \tag{3.2}$$

For PNC, relay node transmits the signal after encoding signals from two end nodes. Hence, it is needless to detect signal separately and is suitable to detect the signal based on the XOR criterion. Let $b = b_1 \bigoplus b_2$ be the network codeword. Then, the relay detect b and forward it back to the end nodes. In this case, although we have four possible for (b_1, b_2), b have only two possible values and our detection problem becomes a binary hypothesis testing problem. It has been shown that the optimal detection scheme for a binary hypothesis testing problem is the likelihood ratio test (LRT) [14].

From (16) of [14], an equivalent optimal test is

$$\Lambda(b) \stackrel{\Delta}{=} \log \left\{ \frac{P_r(\mathbf{y}|b=1)}{P_r(\mathbf{y}|b=0)} \right\} \underset{0}{\overset{1}{\gtrless}} 0$$

because $P_r(b_i = 0) = P_r(b_i = 1) = \frac{1}{2}$. Do notice that

$$\begin{aligned}
\Lambda(b) &= \log\left\{\frac{P_r(\mathbf{y}|b_1 \oplus b_2 = 1)}{P_r(\mathbf{y}|b_1 \oplus b_2 = 0)}\right\} \\
&= \log\left\{\frac{P_r(\mathbf{y}|\mathbb{E}_3 \bigcup \mathbb{E}_4)}{P_r(\mathbf{y}|\mathbb{E}_1 \bigcup \mathbb{E}_2)}\right\} \\
&= \log\left\{\frac{P_r(\mathbf{y}|\mathbb{E}_3) + P_r(\mathbf{y}|\mathbb{E}_4)}{P_r(\mathbf{y}|\mathbb{E}_1) + P_r(\mathbf{y}|\mathbb{E}_2)}\right\} \\
&= \log\{p(\mathbf{y}|\mathbb{E}_3) + p(\mathbf{y}|\mathbb{E}_4)\} - \log\{p(\mathbf{y}|\mathbb{E}_1) + p(\mathbf{y}|\mathbb{E}_2)\} \qquad (3.3)
\end{aligned}$$

As can be seen, the optimal detector requires the computation of $p(\mathbf{y}|\mathbb{E}_i)$ and $p(\mathbf{y}|\mathbb{E}_i)$ depends on the system model. Hence, the computation of each $p(\mathbf{y}|\mathbb{E}_i)$ is done in the following section according to the system model discussed in the last chapter.

3.1 Detection schemes in case 1

3.1.1 The optimal detection scheme in case 1

In this section, we find the conditional probability density function (pdf) of $\mathbb{E}_i$, $i = 1, \cdots, 4$. Recall that. under perfect timing alignment, the equivalent baseband signal is (2.2) and based on a event $\mathbb{E}_i$, the signal part is shown in (2.4).

For $\mathbb{E}_1$, we have $y_1 = h_1 + h_2 + n_1$ and $y_2 = n_2$. Since the channel coefficients are assumed to be the zero mean complex Gaussian random variables with variance depending on the transmission power of source nodes, y_1 is the sum of three independent complex Gaussian random variable. The distribution of y_1 can be easily obtained by the following lemma.

Lemma 3.1.1. *For two independent zero mean complex Gaussian random variables x and y with variance σ_x and σ_y, respectively, the distribution of $z = x + y$ is also zero mean complex Gaussian random variables with variance $\sigma_x + \sigma_y$.*

For convenience, we denote a complex Gaussian random variable with mean m and variance σ^2 by $CN(m, \sigma^2)$. Then, according to lemma (3.1.1), the distribution of y_1

is $CN(0, P_{s1} + P_{s2} + N_0)$. Since y_2 only contain the noise, the distribution of y_2 is $CN(0, N_0)$.

Similarly, with the aid of lemma 3.1.1, the distribution of y_1 and y_2 under various events are summary in the following table. The joint distribution of y_1 and y_2 under

Table 3.1: The distribution of y_1 and y_2 under various events

Event	y_1	y_2
$\mathbb{E}_1$	$CN(0, P_{s1} + P_{s2} + N_0)$	$CN(0, N_0)$
$\mathbb{E}_2$	$CN(0, N_0)$	$CN(0, P_{s1} + P_{s2} + N_0)$
$\mathbb{E}_3$	$CN(0, P_{s1} + N_0)$	$CN(0, P_{s2} + N_0)$
$\mathbb{E}_4$	$CN(0, P_{s2} + N_0)$	$CN(0, P_{s1} + N_0)$

event $\mathbb{E}_i$ is the product of the two distributions because y_1 and y_2 are independent. Hence, the log-likelihood ratio (LLR) (3.3) becomes

$$\begin{aligned}\Lambda(b) &= \log\left(\frac{N_0(N_0+P_{s1}+P_{s2})}{(N_0+P_{s1})(N_0+P_{s2})}\right)\\ &- \log\left(\exp\left\{-\frac{|y_1|^2}{N_0+P_{s1}+P_{s2}}-\frac{|y_2|^2}{N_0}\right\}+\exp\left\{-\frac{|y_2|^2}{N_0+P_{s1}+P_{s2}}-\frac{|y_1|^2}{N_0}\right\}\right)\\ &+ \log\left(\exp\left\{-\frac{|y_1|^2}{N_0+P_{s1}}-\frac{|y_2|^2}{N_0+P_{s2}}\right\}+\exp\left\{-\frac{|y_1|^2}{N_0+P_{s2}}-\frac{|y_2|^2}{N_0+P_{s1}}\right\}\right) \quad (3.4)\end{aligned}$$

3.1.2 Suboptimal detectors in case 1

The optimal detector has been shown in (3.3) and (3.4). In practical, it is hard to implement the detector due to the computation of $\log(\exp(-x)+\exp(-y))$ for some x, $y \in \mathbb{R}$, especially large x or y. To overcome this problem, the computation is approximated by the max-log approximation [15]:

$$\log\left(\exp(-x)+\exp(-y)\right) \approx -\min(x, y).$$

Using this approximation, we have

$$
\begin{aligned}
& -\log\left(\exp\left\{-\frac{|y_1|^2}{N_0+P_{s1}+P_{s2}}-\frac{|y_2|^2}{N_0}\right\}+\exp\left\{-\frac{|y_2|^2}{N_0+P_{s1}+P_{s2}}-\frac{|y_1|^2}{N_0}\right\}\right) \\
= \;& \min\left(\frac{|y_1|^2}{N_0+P_{s1}+P_{s2}}+\frac{|y_2|^2}{N_0},\frac{|y_2|^2}{N_0+P_{s1}+P_{s2}}+\frac{|y_1|^2}{N_0}\right) \qquad (3.5) \\
& \log\left(\exp\left\{-\frac{|y_1|^2}{N_0+P_{s1}}-\frac{|y_2|^2}{N_0+P_{s2}}\right\}+\exp\left\{-\frac{|y_1|^2}{N_0+P_{s2}}-\frac{|y_2|^2}{N_0+P_{s1}}\right\}\right) \\
= \;& -\min\left(\frac{|y_1|^2}{N_0+P_{s1}}+\frac{|y_2|^2}{N_0+P_{s2}},\frac{|y_1|^2}{N_0+P_{s2}}+\frac{|y_2|^2}{N_0+P_{s1}}\right) \qquad (3.6)
\end{aligned}
$$

and (3.4) becomes

$$
\begin{aligned}
\Lambda(b) \;\approx\; & \log\left(\frac{N_0(N_0+P_{s1}+P_{s2})}{(N_0+P_{s1})(N_0+P_{s2})}\right) \\
+ \;& \min\left(\frac{|y_1|^2}{N_0+P_{s1}+P_{s2}}+\frac{|y_2|^2}{N_0},\frac{|y_2|^2}{N_0+P_{s1}+P_{s2}}+\frac{|y_1|^2}{N_0}\right) \\
- \;& \min\left(\frac{|y_1|^2}{N_0+P_{s1}}+\frac{|y_2|^2}{N_0+P_{s2}},\frac{|y_1|^2}{N_0+P_{s2}}+\frac{|y_2|^2}{N_0+P_{s1}}\right) \qquad (3.7)
\end{aligned}
$$

To be concise, we define $\xi = N_0 + P_{s1} + P_{s2}$ and observe that

$$
\begin{aligned}
& \min\left(\frac{|y_1|^2}{N_0+P_{s1}+P_{s2}}+\frac{|y_2|^2}{N_0},\frac{|y_2|^2}{N_0+P_{s1}+P_{s2}}+\frac{|y_1|^2}{N_0}\right) \\
= \;& \min\left(\frac{N_0|y_1|^2+\xi|y_2|^2}{N_0\xi},\frac{\xi|y_1|^2+N_0|y_2|^2}{N_0\xi}\right) \\
= \;& \begin{cases} \frac{N_0|y_1|^2+\xi|y_2|^2}{N_0\xi} & \text{if } |y_1|^2 > |y_2|^2 \\ \frac{\xi|y_1|^2+N_0|y_2|^2}{N_0\xi} & \text{otherwise} \end{cases} \qquad (3.8)
\end{aligned}
$$

Define $x_M = \max(|y_1|^2, |y_2|^2)$ and $x_m = \min(|y_1|^2, |y_2|^2)$. Then, (3.8) becomes

$$
\begin{aligned}
& \min\left(\frac{|y_1|^2}{N_0+P_{s1}+P_{s2}}+\frac{|y_2|^2}{N_0},\frac{|y_2|^2}{N_0+P_{s1}+P_{s2}}+\frac{|y_1|^2}{N_0}\right) \\
= \;& \frac{\xi x_m + N_0 x_M}{N_0\xi} = \frac{x_m}{N_0}+\frac{x_M}{\xi} \qquad (3.9)
\end{aligned}
$$

Similarly, let $\xi_1 = N_0 + P_{s1}$, $\xi_2 = N_0 + P_{s2}$ and

$$
\begin{aligned}
& \min\left(\frac{|y_1|^2}{N_0+P_{s1}}+\frac{|y_2|^2}{N_0+P_{s2}},\frac{|y_1|^2}{N_0+P_{s2}}+\frac{|y_2|^2}{N_0+P_{s1}}\right) \\
= \;& \min\left(\frac{\xi_2|y_1|^2+\xi_1|y_2|^2}{\xi_1\xi_2},\frac{\xi_1|y_1|^2+\xi_2|y_2|^2}{\xi_1\xi_2}\right) \\
= \;& \begin{cases} \frac{\xi_2|y_1|^2+\xi_1|y_2|^2}{\xi_1\xi_2} & (\xi_2-\xi_1)(|y_1|^2-|y_2|^2)<0 \\ \frac{\xi_1|y_1|^2+\xi_2|y_2|^2}{\xi_1\xi_2} & \text{otherwise} \end{cases} \qquad (3.10)
\end{aligned}
$$

Suppose $\xi_M = \max(\xi_1, \xi_2)$ and $\xi_m = \min(\xi_1, \xi_2)$. (3.10) can be further reduced to be

$$\begin{aligned} & \min\left(\frac{|y_1|^2}{N_0+P_{s1}} + \frac{|y_2|^2}{N_0+P_{s2}}, \frac{|y_1|^2}{N_0+P_{s2}} + \frac{|y_2|^2}{N_0+P_{s1}}\right) \\ = \quad & \frac{\xi_M x_m + \xi_m x_M}{\xi_M \xi_m} = \frac{x_M}{\xi_M} + \frac{x_m}{\xi_m} \end{aligned} \tag{3.11}$$

Substituting (3.9) and (3.11) into (3.7), we have

$$\begin{aligned} \Lambda(b) &\approx \log\left(\frac{N_0\xi}{(N_0+\xi_1)(N_0+\xi_2)}\right) + \frac{x_m}{N_0} + \frac{x_M}{\xi} - \frac{x_M}{\xi_M} - \frac{x_m}{\xi_m} \\ &= K + \left(\frac{1}{N_0} - \frac{1}{\xi_m}\right) x_m + \left(\frac{1}{\xi} - \frac{1}{\xi_M}\right) x_M \\ &= K + k_m x_m + k_M x_M \end{aligned} \tag{3.12}$$

where $K = \log\left(\frac{N_0\xi}{(N_0+\xi_1)(N_0+\xi_2)}\right)$, $k_m = \left(\frac{1}{N_0} - \frac{1}{\xi_m}\right)$ and $k_M = \left(\frac{1}{\xi} - \frac{1}{\xi_M}\right)$. Hence, the suboptimal detector is

$$k_m x_m + k_M x_M \underset{0}{\overset{1}{\gtrless}} -K \triangleq \eta \tag{3.13}$$

where $\eta = \log\left(\frac{(N_0+\xi_1)(N_0+\xi_2)}{N_0\xi}\right) = \log\left(\frac{N_0^2+N_0P_{s1}+N_0P_{s2}+P_{s1}P_{s2}}{N_0^2+N_0P_{s1}+N_0P_{s2}}\right) \geq 0$

Do notice that $k_m > 0$ because $\frac{\xi_m - N_0}{N_0\xi_m} = \frac{\min(P_{s1},P_{s2})}{N_0\xi_m} > 0$. Moreover, $k_M < 0$ as $\frac{\xi_M - \xi}{\xi\xi_M} = \frac{-\min(P_{s1},P_{s2})}{\xi\xi_M} < 0$. These two factors will be used when the error rate formula is derived.

As can be seen from (3.13), it depends on x_M and x_m. However, when N_0 goes to zero, the term k_m is larger compared with k_M and is the dominant term. It motives us to further approximate the LLR by omitting the term $k_M x_M$ and we get the second suboptimal detector:

$$k_m x_m \underset{0}{\overset{1}{\gtrless}} \eta \tag{3.14}$$

Later, we will show that these two suboptimal detectors yield negligible performance loss by simulations, hence, the performance analysis is based on these two detectors and is provided in the next section.

3.2 The optimal detection scheme in case 2

From (3.3), to find the optimal detector, the distributions of received signal $\mathbf{y}$ under various events are required. In case 2, to find the distributions is more complex than that in case 1. The difficulty comes from the cross terms due to the timing asynchronization. For example, for event $\mathbb{E}_1$, we have

$$\mathbf{m}_1 = h_1(1-|\epsilon_1|)\begin{bmatrix} 1 \\ e^{-j\pi(1+\epsilon_1)}\text{sinc}(1-|\epsilon_1|) \end{bmatrix} + h_2(1-|\epsilon_2|)\begin{bmatrix} 1 \\ e^{-j\pi(1+\epsilon_2)}\text{sinc}(1-|\epsilon_2|) \end{bmatrix}$$

from (2.11). The distribution of y_1 and y_2 are no longer independent and we should take y_1 and y_2 into account together.

The distributions of received signal $\mathbf{y}$ under various events can be represented as

$$p(\mathbf{y}|\mathbb{E}_i) = \int_{h_2}\int_{h_1} \frac{1}{\pi N_0}\exp\left\{-\frac{1}{N_0}\|\mathbf{y}-\mathbf{m}_i\|^2\right\} f(h_1)f(h_2)dh_1dh_2$$

where $\mathbf{m}_i$ are described by (2.11).

Expanding the above equation, we have

$$\begin{aligned} p(\mathbf{y}|\mathbb{E}_i) &= \int_{h_2}\int_{h_1} \frac{1}{\pi N_0}\exp\left\{-\frac{1}{N_0}\left[|y_1-(1-|\epsilon_1|)t_{11}h_1-(1-|\epsilon_2|)t_{12}h_2|^2\right.\right. \\ &\quad \left.\left.+|y_2-(1-|\epsilon_1|)t_{21}h_1-(1-|\epsilon_2|)t_{22}h_2|^2\right]\right\} f(h_1)f(h_2)dh_1dh_2 \\ &= \int_{h_2}\int_{h_1} \frac{1}{\pi N_0}\exp\left\{-\frac{1}{N_0}\left[|y_1'-(1-|\epsilon_1|)t_{11}h_1|^2+|y_2'-(1-|\epsilon_1|)t_{21}h_1|^2\right]\right\} \\ &\quad f(h_1)f(h_2)dh_1dh_2 \end{aligned} \tag{3.15}$$

where

$$y_1' = y_1-(1-|\epsilon_2|)t_{12}h_2 \quad , \quad y_2' = y_2-(1-|\epsilon_2|)t_{22}h_2$$

and t_{11}, t_{12}, t_{21}, t_{22} are constants depending on the timing offset and events. The value of t_{11}, t_{12}, t_{21}, and t_{22} under various events are summary in Table 3.2, where $t_1 = \text{sinc}(1-|\epsilon_1|)$, $t_2 == \text{sinc}(1-|\epsilon_2|)$.

In the remaining part of this section, we will find out the distribution case by case and the optimal detector can be found with these results and (3.3).

To integrate h_1, We need the following useful lemma 3.2.1.

Table 3.2: The value of t_{11}, t_{12}, t_{21}, and t_{22} under various events

Event	t_{11}	t_{12}	t_{21}	t_{22}
$\mathbb{E}_1$	1	1	$t_1 \exp\{-j\pi(1+\epsilon_1)\}$	$t_2 \exp\{-j\pi(1+\epsilon_2)\}$
$\mathbb{E}_2$	$t_1 \exp\{j\pi(1+\epsilon_1)\}$	$t_2 \exp\{j\pi(1+\epsilon_2)\}$	1	1
$\mathbb{E}_3$	1	$t_2 \exp\{j\pi(1+\epsilon_2)\}$	$t_1 \exp\{-j\pi(1+\epsilon_1)\}$	1
$\mathbb{E}_4$	$t_1 \exp\{j\pi(1+\epsilon_1)\}$	1	1	$t_2 \exp\{-j\pi(1+\epsilon_2)\}$

Lemma 3.2.1. *Suppose h is a zero mean complex Gaussian random variable with variance σ_h^2, then*

$$\int_h \exp\left\{-\frac{|y-h|^2}{N_0}\right\} f(h)dh = \frac{N_0}{N_0+\sigma_h^2} \exp\left\{-\frac{|y|^2}{N_0+\sigma_h^2}\right\} \tag{3.16}$$

Proof. The proof of this lemma is shown in Appendix. □

For convenience, (3.15) is repeated below.

$$\begin{aligned} & p(\mathbf{y}|\mathbb{E}_i) \\ = & \int_{h_2}\int_{h_1} \frac{1}{\pi N_0} \exp\left\{-\frac{1}{N_0}\left[|y_1' - (1-|\epsilon_1|)t_{11}h_1|^2 + |y_2' - (1-|\epsilon_1|)t_{21}h_1|^2\right]\right\} f(h_1)f(h_2)dh_1dh_2 \end{aligned}$$

Observe that

$$\begin{aligned} & |y_1' - (1-|\epsilon_1|)t_{11}h_1|^2 + |y_2' - (1-|\epsilon_1|)t_{21}h_1|^2 \\ = & |h_1|^2\left((|t_{11}|^2+|t_{21}|^2)(1-|\epsilon_1|)^2\right) + 2(1-|\epsilon_1|)\Re\{y_1'^* t_{11}h_1 + y_2'^* t_{21}h_1\} + |y_1'|^2 + |y_2'|^2 \\ = & (|t_{11}|^2+|t_{21}|^2)\left|(1-\epsilon_1)h_1 - \frac{y_2't_{21}^* + y_1't_{11}^*}{|t_{11}|^2+|t_{21}|^2}\right|^2 - \frac{|y_1't_{11}^* + y_2't_{21}^*|^2}{|t_{11}|^2+|t_{21}|^2} + |y_1'|^2 + |y_2'|^2 \\ = & (|t_{11}|^2+|t_{21}|^2)\left|(1-\epsilon_1)h_1 - \frac{y_2't_{21}^* + y_1't_{11}^*}{|t_{11}|^2+|t_{21}|^2}\right|^2 + \frac{|y_2't_{11} - y_1't_{21}|^2}{|t_{11}|^2+|t_{21}|^2} \end{aligned}$$

Hence, the distribution of $\mathbf{y}$ given $\mathbb{E}_i$ is

$$\begin{aligned} p(\mathbf{y}|\mathbb{E}_i) = & \int_{h_2}\frac{1}{\pi N_0}\int_{h_1}\exp\left\{-\frac{1}{N_0}\left[(|t_{11}|^2+|t_{21}|^2)\left|(1-\epsilon_1)h_1 - \frac{y_2't_{21}^* + y_1't_{11}^*}{|t_{11}|^2+|t_{21}|^2}\right|^2 + \frac{|y_2't_{11}-y_1't_{21}|^2}{|t_{11}|^2+|t_{21}|^2}\right]\right\} \\ & f(h_1)f(h_2)dh_1dh_2 \\ = & \int_{h_2}\frac{1}{\pi N_0}\exp\left\{-\frac{|y_2't_{11}-y_1't_{21}|^2}{N_0(|t_{11}|^2+|t_{21}|^2)}\right\} \\ & \int_{h_1}\exp\left\{-\frac{1}{N_0/(|t_{11}|^2+|t_{21}|^2)}\left|(1-|\epsilon_1|)h_1 - \frac{y_2't_{21}^* + y_1't_{11}^*}{|t_{11}|^2+|t_{21}|^2}\right|^2\right\} f(h_1)f(h_2)dh_1dh_2 \end{aligned}$$

Let $h_1' = (1-|\epsilon_1|)h_1$. Then, according to lemma 3.2.1, we have

$$\begin{aligned}
& p(\mathbf{y}|\mathbb{E}_i) \\
= & \int_{h_2} \frac{1}{\pi N_0} \exp\left\{-\frac{|y_2' t_{11} - y_1' t_{21}|^2}{N_0(|t_{11}|^2+|t_{21}|^2)}\right\} \frac{N_0/(|t_{11}|^2+|t_{21}|^2)}{N_0/(|t_{11}|^2+|t_{21}|^2)+(1-|\epsilon_1|)^2 P_{s1}} \\
& \exp\left\{-\frac{\left|\frac{y_2' t_{21}^* + y_1' t_{11}^*}{|t_{11}|^2+|t_{21}|^2}\right|^2}{N_0/(|t_{11}|^2+|t_{21}|^2)+(1-|\epsilon_1|)^2 P_{s1}}\right\} f(h_2) dh_2 \\
= & \int_{h_2} \frac{1}{\pi} \frac{1}{N_0 + T_1 K_1} \exp\left\{-\frac{|y_2' t_{11} - y_1' t_{21}|^2}{N_0 T_1} - \frac{|y_2' t_{21}^* + y_1' t_{11}^*|^2}{N_0 T_1 + T_1^2 K_1}\right\} f(h_2) dh_2 \qquad (3.17)
\end{aligned}$$

where $K_1 = (1-|\epsilon_1|)^2 P_{s1}$ and $T_1 = |t_{11}|^2 + |t_{21}|^2$. Similarly, we want to integrate h_2 via the lemma 3.2.1. Again, we observe that

$$\begin{aligned}
& \frac{|y_2' t_{11} - y_1' t_{21}|^2}{N_0 T_1} + \frac{|y_2' t_{21}^* + y_1' t_{11}^*|^2}{N_0 T_1 + T_1^2 K_1} \\
= & \frac{1}{T_1}\left[\frac{|y_2' t_{11} - y_1' t_{21}|^2}{N_0} + \frac{|y_2' t_{21}^* + y_1' t_{11}^*|^2}{N_0 + T_1 K_1}\right] \\
= & \frac{1}{T_1} \frac{T_1 K_1 (|y_2' t_{11} - y_1' t_{21}|^2) + N_0(|y_2' t_{21}^*|^2 + |y_1' t_{11}^*|^2 + |y_2' t_{11}|^2 + |y_1' t_{21}|^2)}{N_0(N_0 + T_1 K_1)} \\
= & \frac{K_1(|y_2' t_{11} - y_1' t_{21}|^2) + N_0(|y_2'|^2 + |y_1'|^2)}{N_0(N_0 + T_1 K_1)}
\end{aligned}$$

Recall that

$$y_1' = y_1 - (1-|\epsilon_2|)t_{12}h_2, \qquad y_2' = y_2 - (1-|\epsilon_2|)t_{22}h_2$$

Then, we have

$$\begin{aligned}
& \frac{|y_2' t_{11} - y_1' t_{21}|^2}{N_0 T_1} + \frac{|y_2' t_{21}^* + y_1' t_{11}^*|^2}{N_0 T_1 + T_1^2 K_1} \\
= & \frac{K_1(|(y_2 - (1-|\epsilon_2|)t_{22}h_2)t_{11} - (y_1 - (1-|\epsilon_2|)t_{12}h_2)t_{21}|^2)}{N_0(N_0 + T_1 K_1)} \\
+ & \frac{N_0(|y_2 - (1-|\epsilon_2|)t_{22}h_2|^2 + |y_1 - (1-|\epsilon_2|)t_{12}h_2|^2)}{N_0(N_0 + T_1 K_1)} \qquad (3.18)
\end{aligned}$$

The numerator can be represented as

$$
\begin{aligned}
& K_1(|(y_2-(1-|\epsilon_2|)t_{22}h_2)t_{11}-(y_1-(1-|\epsilon_2|)t_{12}h_2)t_{21}|^2) \\
& +N_0(|y_2-(1-|\epsilon_2|)t_{22}h_2|^2+|y_1-(1-|\epsilon_2|)t_{12}h_2|^2) \\
= \;& K_1|(y_2t_{11}-y_1t_{21})-(1-|\epsilon_2|)(t_{11}t_{22}-t_{12}t_{21})h_2|^2 \\
& +N_0|y_2-(1-|\epsilon_2|)t_{22}h_2|^2+N_0|y_1-(1-|\epsilon_2|)t_{12}h_2|^2 \\
= \;& K_1|y_2t_{11}-y_1t_{21}|^2+K_1(1-|\epsilon_2|)^2|t_{11}t_{22}-t_{12}t_{21}|^2|h_2|^2 \\
& -2K_1(1-|\epsilon_2|)\Re\{(y_2t_{11}-y_1t_{21})^*(t_{11}t_{22}-t_{12}t_{21})h_2\} \\
& +N_0|y_2|^2+N_0|y_1|^2+N_0(1-|\epsilon_2|)^2(|t_{12}|^2+|t_{22}|^2)|h_2|^2-2N_0(1-|\epsilon_2|)\Re\{y_2^*t_{22}h_2+y_1^*t_{12}h_2\} \\
= \;& K_1|y_2t_{11}-y_1t_{21}|^2+N_0|y_2|^2+N_0|y_1|^2+\{K_1|t_{11}t_{22}-t_{12}t_{21}|^2+N_0(|t_{12}|^2+|t_{22}|^2)\}(1-|\epsilon_2|)^2|h_2|^2 \\
& -2(1-|\epsilon_2|)\Re\{[K_1(y_2t_{11}-y_1t_{21})^*(t_{11}t_{22}-t_{12}t_{21})+N_0(y_2^*t_{22}+y_1^*t_{12})]h_2\} \\
= \;& M_i\left|(1-|\epsilon_2|)h_2-\frac{A_i}{M_i}\right|^2-\frac{|A_i|^2}{M_i}+B_i
\end{aligned}
\tag{3.19}
$$

where

$$
\begin{aligned}
M_i &= K_1|t_{11}t_{22}-t_{12}t_{21}|^2+N_0(|t_{12}|^2+|t_{22}|^2) \\
A_i &= K_1(y_2t_{11}-y_1t_{21})(t_{11}t_{22}-t_{12}t_{21})^*+N_0(y_2t_{22}^*+y_1t_{12}^*) \\
B_i &= K_1|y_2t_{11}-y_1t_{21}|^2+N_0|y_2|^2+N_0|y_1|^2
\end{aligned}
$$

Let $G=N_0+T_1K_1$ and $K_2=(1-|\epsilon_2|)^2P_{s2}$. With (3.17)-(3.19) and lemma 3.2.1, we have

$$
\begin{aligned}
p(\mathbf{y}|\mathbb{E}_i) &= \int_{h_2}\frac{1}{\pi G}\exp\left\{-\frac{M_i\left|(1-|\epsilon_2|)h_2-\frac{A_i}{M_i}\right|^2-\frac{|A_i|^2}{M_i}+B_i}{N_0G}\right\}f(h_2)dh_2 \\
&= \frac{1}{\pi G}\exp\left\{\frac{|A_i|^2}{M_iN_0G}-\frac{B_i}{N_0G}\right\}\int_{h_2}\exp\left\{-\frac{1}{N_0G/M_i}\left|(1-|\epsilon_2|)h_2-\frac{A_i}{M_i}\right|^2\right\}f(h_2)dh_2 \\
&= \frac{1}{\pi G}\frac{N_0G/M_i}{N_0G/M_i+K_2}\exp\left\{-\frac{\left|\frac{A_i}{M_i}\right|^2}{N_0G/M_i+K_2}+\frac{|A_i|^2}{M_iN_0G}-\frac{B_i}{N_0G}\right\} \\
&= \frac{1}{\pi}\frac{N_0}{N_0G+K_2M_i}\exp\left\{\frac{K_2|A_i|^2}{(N_0G+K_2M_i)N_0G}-\frac{B_i}{N_0G}\right\}
\end{aligned}
\tag{3.20}
$$

Hence, the condition pdf (3.20) for each event can be obtained by substitute each different t_{11},t_{12}, t_{21}, and t_{22} in Table 3.2 and the parameters involved in (3.20) are summary in Table 3.3.

Table 3.3: The parameters involved in (3.20)

General term	
$K_1 = (1-\|\epsilon_1\|)^2 P_{s1}$, $K_2 = (1-\|\epsilon_2\|)^2 P_{s2}$ $t_1 = \text{sinc}(1-\|\epsilon_1\|)$, $t_2 = \text{sinc}(1-\|\epsilon_2\|)$ $G = N_0 + T_1 K_1$, $T_1 = \|t_{11}\|^2 + \|t_{21}\|^2$	
Event	M
$\mathbb{E}_1$	$K_1\|t_{22}-t_{21}\|^2 + N_0(\|t_{22}\|^2+1)$
$\mathbb{E}_2$	$K_1\|t_{11}-t_{12}\|^2 + N_0(\|t_{12}\|^2+1)$
$\mathbb{E}_3$	$K_1\|1-t_{12}t_{21}\|^2 + N_0(1+\|t_{12}\|^2)$
$\mathbb{E}_4$	$K_1\|1-t_{22}t_{11}\|^2 + N_0(1+\|t_{22}\|^2)$
Event	A
$\mathbb{E}_1$	$K_1(y_2-y_1t_{21})(t_{22}-t_{21})^* + N_0(y_2t_{22}^* + y_1)$
$\mathbb{E}_2$	$K_1(y_1-y_2t_{11})(t_{12}-t_{11})^* + N_0(y_1t_{12}^* + y_2)$
$\mathbb{E}_3$	$K_1(y_2-y_1t_{21})(1-t_{12}t_{21})^* + N_0(y_2+y_1t_{12}^*)$
$\mathbb{E}_4$	$K_1(y_1-y_2t_{11})(1-t_{22}t_{11})^* + N_0(y_1+y_2t_{22}^*)$
Event	B
$\mathbb{E}_1$, $\mathbb{E}_3$	$K_1\|y_2-y_1t_{21}\|^2 + N_0\|y_2\|^2 + N_0\|y_1\|^2$
$\mathbb{E}_2$, $\mathbb{E}_4$	$K_1\|y_1-y_2t_{11}\|^2 + N_0\|y_1\|^2 + N_0\|y_2\|^2$

Chapter 4

Bit error rate of receiver over Rayleigh fading channel

4.1 Bit error rate of the two suboptimal detectors in case 1

In the next section, we will show that these two suboptimal detectors in case 1 have the performance similar to that of the optimal scheme. Therefore, it motives us to consider the performance analysis of these two suboptimal detectors. Do notice that these two detectors not only avoid the numerical sensitivity problem, but the performance analysis of these two detectors are easiler than that of optimal detector because they have a simple representation.

4.1.1 Bit error rate of the first suboptimal detector in case 1

Recall that the first suboptimal detector is

$$k_m x_m + k_M x_M \underset{0}{\overset{1}{\gtrless}} \eta \tag{4.1}$$

and $x_m = \min(|y_1|^2, |y_2|^2)$, $x_M = \max(|y_1|^2, |y_2|^2)$ and its bit error rate (BER) is

$$P_e = \frac{1}{2} P_e(k_m x_m + k_M x_M < \eta | b = 1) + \frac{1}{2} P_e(k_m x_m + k_M x_M > \eta | b = 0). \tag{4.2}$$

In fact, the following theorem states the BER formula for the first suboptimal detector.

Theorem 4.1.1. *The BER of the first suboptimal detector is*

$$P_e = \frac{1}{2}\left(1 - P_e(k_m x_m + k_M x_M > \eta | b = 1) + P_e(k_m x_m + k_M x_M > \eta | b = 0)\right) \quad (4.3)$$

where

$$\begin{aligned} & P_e(k_m x_m + k_M x_M > \eta | b = 1) \\ = \; & k_m \lambda \left(\frac{N_0 \xi}{\xi_1 \xi_2}\right)^{\frac{1}{k_m \lambda}} \left(\frac{1}{|k_M|\xi_1 + k_m \lambda} + \frac{1}{|k_M|\xi_2 + k_m \lambda} - \frac{1}{|k_M|\lambda + k_m \lambda}\right), \\ \lambda = \; & \frac{\xi_1 \xi_2}{\xi_1 + \xi_2} \end{aligned} \quad (4.4)$$

and

$$\begin{aligned} & P_e(k_m x_m + k_M x_M > \eta | b = 0) \\ = \; & k_m \lambda \left(\frac{N_0 \xi}{\xi_1 \xi_2}\right)^{\frac{1}{k_m \lambda}} \left(\frac{1}{|k_M|\xi + k_m \lambda} + \frac{1}{|k_M|N_0 + k_m \lambda} - \frac{1}{|k_M|\lambda + k_m \lambda}\right), \\ \lambda = \; & \frac{\xi N_0}{\xi + N_0} \end{aligned} \quad (4.5)$$

Proof. To derive the bit error rate, we need to find the distribution of $k_m x_m + k_M x_M$ under $b = 0$ or $b = 1$. As shown in Table 3.1, the distribution of y_1 and y_2 are zero mean complex Gaussian random variable with variance depending on the considered event. Hence, $|y_1|^2$ and $|y_2|^2$ are exponential random variables. Specifically, suppose x is $CN(0, \sigma_x)$, then, $|x|^2$ is a exponential random variable with mean σ_x (denoted by $exponential(\sigma_x)$) [16].

Before completing the proof, we need the following two lemmas and their proofs are provided in the appendix.

Lemma 4.1.2. *Suppose $x_1 \sim exponential(\lambda_1)$, $x_2 \sim exponential(\lambda_2)$ are independent random variables and let $x_M = \max\{x_1, x_2\}$, $x_m = \min\{x_1, x_2\}$. Then, we have*

$$\begin{aligned} f(x_m) &= \frac{\lambda_1 + \lambda_2}{\lambda_1 \lambda_2} \exp\left\{-\frac{\lambda_1 + \lambda_2}{\lambda_1 \lambda_2} x_m\right\}, \; x_m \geq 0 \\ f(x_M) &= \frac{1}{\lambda_1} \exp\left\{-\frac{x_M}{\lambda_1}\right\} + \frac{1}{\lambda_2} \exp\left\{-\frac{x_M}{\lambda_2}\right\} - \frac{\lambda_1 + \lambda_2}{\lambda_1 \lambda_2} \exp\left\{-\frac{\lambda_1 + \lambda_2}{\lambda_1 \lambda_2} x_M\right\}, \; x_M \geq 0 \end{aligned}$$

and

Lemma 4.1.3. *Suppose $x_1 \sim$ exponential(λ_1), $x_2 \sim$ exponential(λ_2). The distributions of $z_s = x_1 + x_2$ and $z_d = x_1 - x_2$ are*

$$\begin{aligned} f(z_s) &= \frac{1}{\lambda_2 - \lambda_1}\left(e^{-\frac{z_s}{\lambda_2}} - e^{-\frac{z_s}{\lambda_1}}\right) \\ f(z_d) &= \begin{cases} \frac{1}{\lambda_1+\lambda_2}\, e^{-\frac{z_d}{\lambda_1}}, & z_d \geq 0 \\ \frac{1}{\lambda_1+\lambda_2}\, e^{\frac{z_d}{\lambda_2}}, & z_d \leq 0 \end{cases} \end{aligned}$$

From the above two lemmas, we are ready to calculate the probability of $L' \triangleq k_M x_M + k_m x_m \leq \eta$. Do notice that

$$\begin{aligned} P_e(k_m x_m + k_M x_M < \eta | b = 1) &= 1 - P_e(k_m x_m + k_M x_M > \eta | b = 1) \\ P_e(k_m x_m + k_M x_M < \eta | b = 0) &= 1 - P_e(k_m x_m + k_M x_M > \eta | b = 0). \end{aligned}$$

Hence, it is sufficient to consider $Pe(L' < \eta | b = 1)$ and $Pe(L' < \eta | b = 0)$. Moreover, it can be seen that L' has the same distribution under $b = 0$ and $b = 1$, and the difference is only the moment of L'; it is sufficient to consider one of the two cases. Then, according to the above two lemmas, we have

$$\begin{aligned} & Pr\{L' \leq \eta | b = 1\} \\ = \; & Pr\{k_m x_m \leq \eta + |k_M| x_M\} \\ = \; & \int_0^\infty \int_0^{\eta + |k_M| x_M} \left(\frac{e^{-\frac{x_M}{|k_M|\xi_1}}}{|k_M|\xi_1} + \frac{e^{-\frac{x_M}{|k_M|\xi_2}}}{|k_M|\xi_2} - \frac{e^{-\frac{x_M}{|k_M|(\frac{\xi_1\xi_2}{\xi_1+\xi_2})}}}{|k_M|\left(\frac{\xi_1\xi_2}{\xi_1+\xi_2}\right)} \right) \frac{\xi_1+\xi_2}{k_m\xi_1\xi_2} e^{-\frac{x_m}{k_m\left(\frac{\xi_1\xi_2}{\xi_1+\xi_2}\right)}} dx_m dx_M \\ = \; & 1 - k_m\lambda e^{-\frac{\eta}{k_m\lambda}} \left(\frac{1}{k_m\lambda + |k_M|\xi_1} + \frac{1}{k_m\lambda + |k_M|\xi_2} - \frac{1}{k_m\lambda + |k_M|\lambda} \right) \end{aligned}$$

where the second line comes from that $k_M < 0$. The third line use the fact that $\eta \geq 0$, lemma 4.1.2 and lemma 4.1.3. λ is defined as $\frac{\xi_1\xi_2}{\xi_1+\xi_2}$. Because $\eta = -K = -log\left(\frac{N_o\xi}{\xi_1\xi_2}\right)$, we have $e^{-\frac{\eta}{k_m\lambda}} = \left(\frac{N_o\xi}{\xi_1\xi_2}\right)^{\frac{1}{k_m\lambda}}$. Hence, we can get (4.4) and (4.5) can be easily obtained by replacing ξ_1 and ξ_2 with ξ and N_0, respectively. □

4.1.2 Bit error rate of the second suboptimal detector in case 1

Recall that the second suboptimal detector is

$$k_m x_m \underset{0}{\overset{1}{\gtrless}} \eta \tag{4.6}$$

Because $k_m > 0$, the detector can be rewritten as

$$x_m \underset{0}{\overset{1}{\gtrless}} \eta/k_m \tag{4.7}$$

As stated in lemma 4.1.2, x_m is a exponential random variable with parameter λ. λ is $\frac{\xi_1\xi_2}{\xi_1+\xi_2}$ under $b=1$ while λ is $\frac{\xi N_0}{\xi+N_0}$ under $b=0$. Hence, the error rate under various cases is

$$\begin{aligned}
P_e\{x_m > \eta/k_m | b=0\} &= \int_{\eta/k_m}^{\infty} f_{x_m}(x)dx = \exp\left\{-\frac{N_0+\xi}{N_0\xi}\eta/k_m\right\} \\
P_e\{x_m < \eta/k_m | b=1\} &= \int_{0}^{\eta/k_m} f_{x_m}(x)dx = 1-\exp\left\{-\frac{\xi_1+\xi_2}{\xi_1\xi_2}\eta/k_m\right\} = 1-P_r\{x_m > C|H_1\}
\end{aligned}$$

and the BER is

$$\begin{aligned}
P_e &= \frac{1}{2}\left(P_e\{x_m > \eta/k_m|b=0\} + P_e\{x_m < \eta/k_m|b=1\}\right) \\
&= \frac{1}{2}\left(\exp\left\{-\frac{N_0+\xi}{N_0\xi}\eta/k_m\right\} + 1 - \exp\left\{-\frac{\xi_1+\xi_2}{\xi_1\xi_2}\eta/k_m\right\}\right) \\
&= \frac{1}{2} + \frac{1}{2}\exp\left\{-\frac{N_0+\xi}{N_0\xi}\frac{\log\left(\xi_1\xi_2/N_0\xi\right)}{1/N_0-1/\xi_m}\right\} - \frac{1}{2}\exp\left\{-\frac{\xi_1+\xi_2}{\xi_1\xi_2}\frac{\log\left(\xi_1\xi_2/N_0\xi\right)}{1/N_0-1/\xi_m}\right\} \\
&= \frac{1}{2} + \frac{1}{2}\left(\frac{\xi_1\xi_2}{N_0\xi}\right)^{-\frac{N_0+\xi}{N_0\xi(1/N_0-1/\xi_m)}} - \frac{1}{2}\left(\frac{\xi_1\xi_2}{N_0\xi}\right)^{-\frac{\xi_1+\xi_2}{\xi_1\xi_2(1/N_0-1/\xi_m)}}
\end{aligned} \tag{4.8}$$

Chapter 5

Simulation/Numerical results

In the following simulations, signal-to-noise ratio (SNR) is define as the total signal power divided by noise power P/N_0, where the total power is the sum of the power from two sources P_{s1}, P_{s2}. To investigate the power loading problem, the power loading factor is denoted by P_{factor} and, without loss of generality, we have $P_{factor} = P_1/P$. The simulation will be stopped if the error occurs more than 1000 times.

5.1 The performance of the optimal and suboptimal detectors in case 1

For convenience. the optimal detector (3.4) is labelled as "opt. detector" in the figure. The suboptimal detectors (3.13) and (3.14) are denoted by "1st subopt." and "2nd subopt.", respectively. Moreover, "analysis 1" and "analysis 2" are abbreviations for the performance analysis of the first and second suboptimal detectors (4.5) and (4.8), respectively.

First, we investigate the performance loss due to the approximation by simulation. As illustrated in Fig. 5.1 with power loading factor $P_{factor} = 0.5$, the BER curves of the optimal detector and the first suboptimal detector are almost identical, especially at high SNR region. Moreover, the simulation result of the first suboptimal detector is identical to the numerical result of (4.5). This justifies our performance analysis.

Figure 5.2 further shows that the performance of the first suboptimal detector can

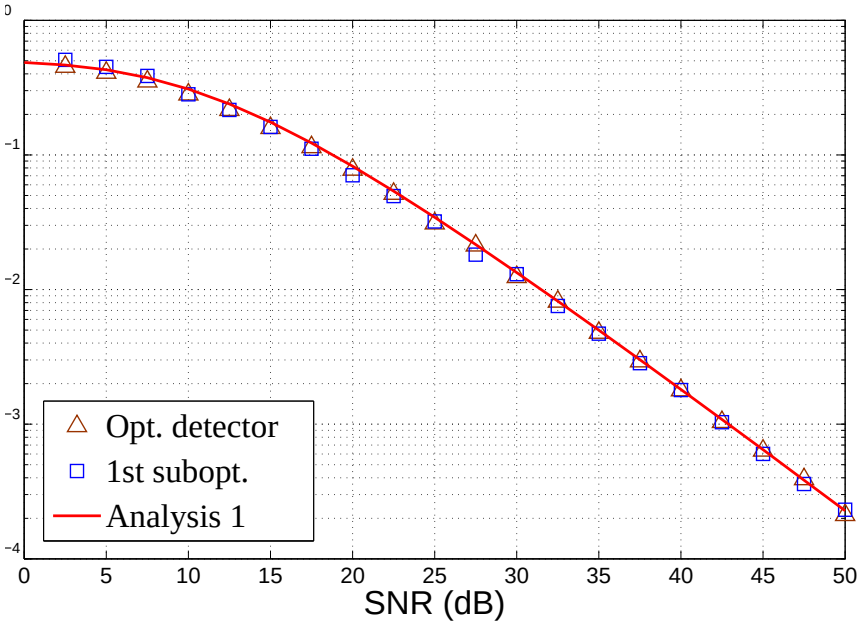

Figure 5.1: Performances of the optimal detector (3.4) and the first suboptimal detector (3.13). The power loading factor is 0.5. The analysis (4.5) is included.

be predicted by (4.5) under various power loading factor P_{factor}, we consider $P_{factor} = 0.5,\ 0.75$ and 0.95. Moreover, we can observe that the optimal power loading is 0.5 among the three cases. It is the future work to show that the optimal power loading is 0.5 or near 0.5 for all power loading analytically. Similarly, Fig. 5.3 shows that the the performance of the second detector under various power loading factors and the same conclusion is obtained. (Because the performance of the first suboptimal detector is similar to that of the optimal detector, we use the result of the analysis as the performance of the optimal detector.)

It is interesting to compare the performance of PNC with that of TPTC system to show which system is more suitable for wireless environment. Recall that, in TPTC system, the two source nodes transmit their messages in orthogonal time slots. The relay receiver first detect the individual signals during each time slot based on the decision

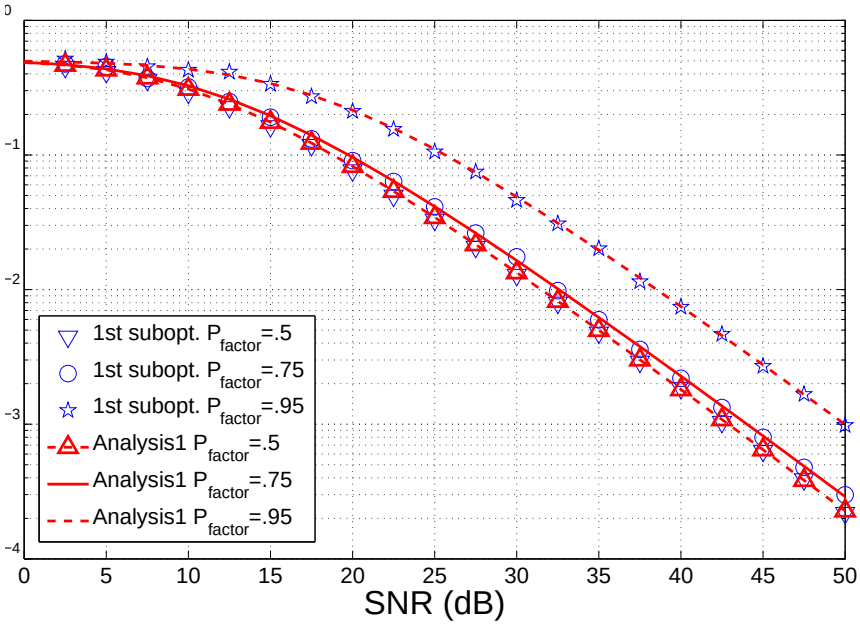

Figure 5.2: Performances of the first suboptimal detector (3.13) with the analysis (4.5) under various power loading factors.

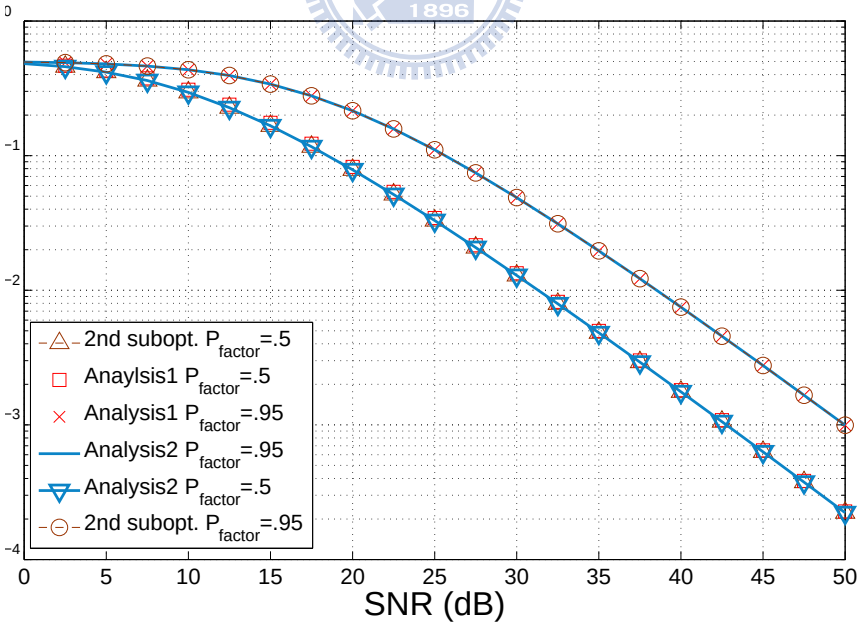

Figure 5.3: Performances of the second suboptimal detector (3.14) with the analysis (4.5) and (4.8) under various power loading factors.

rule

$$\widehat{b}_i = \begin{cases} 0 & \text{if } |y_{1,i}|^2 - |y_{2,i}|^2 > 0 \\ 1 & \text{otherwise} \end{cases}, \tag{5.1}$$

Then, the detection of $\widehat{b}$ is obtained by encoding $\widehat{b}_1$ and $\widehat{b}_2$ according to the XOR rule. Through the detection procedure, an error occurs if only one of the two bits b_1, b_2 is detected incorrectly. Therefore, the error rate of the TPTC system is $P_b^{TPTC} = p_1(1-p_2) + p_2(1-p_1)$, where $p_i = 1/(2 + P_{si}/N_0)$ is the bit error rate of noncoherent binary FSK modulation. However, for TPTC system, it requires two time slots to to transmit the signals and an additional time slot is needed compared with PNC system. To compare these two system in terms of throughput, we consider a packet with length P_l and the normalized throughput is defined as $(1-P_e)^{P_l}/T_p$, where P_e is the bit error rate and T_p is the normalized transmission time of a packet. The normalized throughput is equal to $(1-P_e)^{P_l}$ and $(1-P_b^{TPTC})^{P_l}/2$ for PNC and TPTC, respectively.

$\frac{P}{2N_0}$.

Figure 5.4 shows that the normalized throughput of PNC and TPTC with packet length $P_l = 100,\ 1000$ and 10000. The normalized throughput of PNC is higher than that of TPTC when SNR is higher than a threshold, depending on the packet length. Moreover, when the packet length is small, PNC outperforms TPTC at any SNR.

5.2 The performance of the optimal and mismatch detector in case 2

In this section, we consider the effect of timing asynchronization. At the beginning, we investigate the performance of the optimal detector in case 1 in the present of timing error and this detector is called as mismatch detector. The timing offset ϵ_i can be either modelled as uniform random variables between $[-T_{il}, T_{ih}]$ or a fixed vale T_i, for $i = 1, 2$. The former case occurs when the network synchronization is not perfect and relay does not estimate the timing offset. However, relay can estimate the timing offset and, with the information, the performance may be improved further. Hence, we consider an

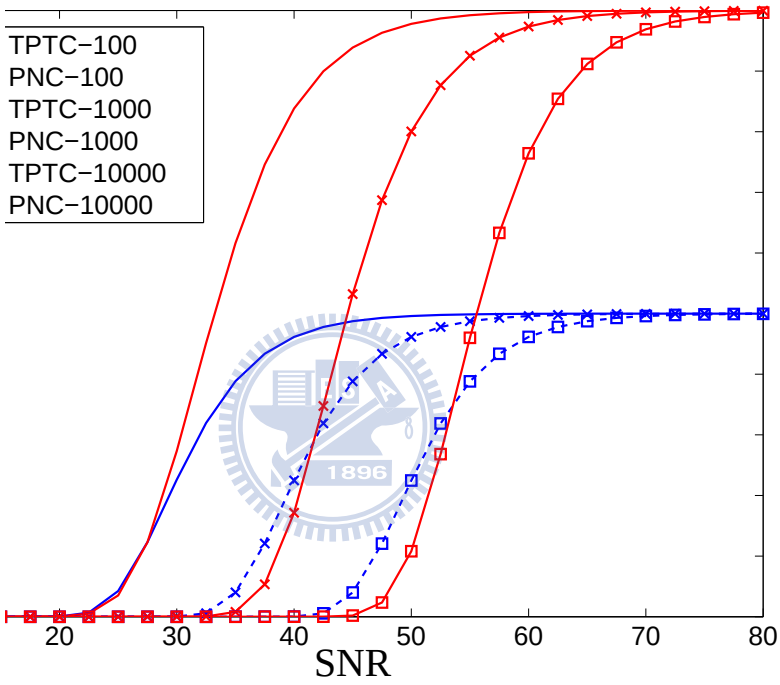

Figure 5.4: The comparison of throughput of PNC and TPTC under different packet length.

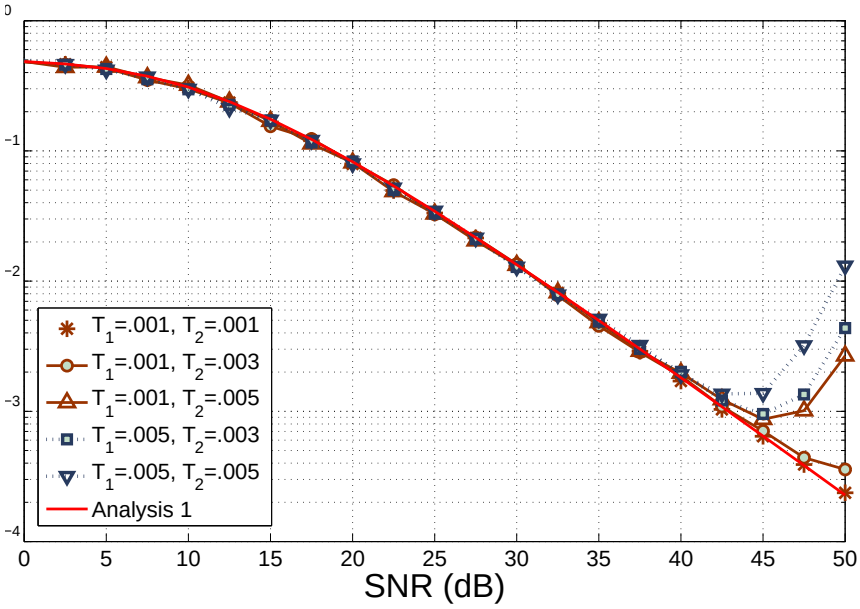

Figure 5.5: The performance of mismatch detector with fixed timing offsets.

extreme case that relay can perfectly estimate the timing offset, which is equal to the later case.

As illustrated in Fig. 5.5, the performance of the mismatch detector with fixed delay is similar to that of the optimal detector without timing offset at low SNR region. However, at high SNR region, the performance of the mismatch detector becomes worse. This phenomena can be explained by observing the structure of the second suboptimal detector. Recall that the structure of the second suboptimal detector is

$$k_m x_m \underset{0}{\overset{1}{\gtrless}} \eta \tag{5.2}$$

It only depends on $x_m = \min(|y_1|^2, |y_2|^2)$. Due to the timing offset, the magnitude of y_1 and y_2 are larger then that of y_1 and y_2 in case 1 (this can be observed in (2.11)). Hence, the suboptimal detector will choose 1 with higher probability at high SNR region. To show this effect, we count the number of $\widehat{b} = 1$ given $b = 0$ in the presence of timing offset or not, as illustrated in Fig. 5.6.

The performance of the mismatch detector with random timing offsets is shown in

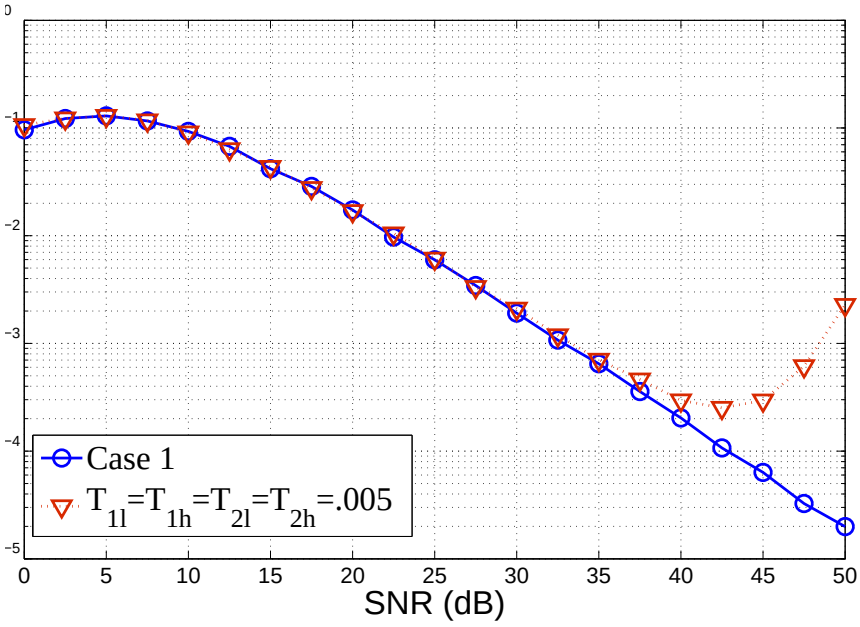

Figure 5.6: The number of $\widehat{b} = 1$ given $b = 0$ in the presence of timing offset or not .

Fig. 5.7. For comparison, the performance of the mismatch detector with fixed timing offsets is also represented. As can be seen, the performance get worse with the increase of timing offsets. Moreover, the performance with rand timing offsets is better that that with fixed timing offsets when $T_{il} = T_{ih} = T_i$, $i = 1, 2$.

Because the mismatch detector has great performance loss at high SNR region, it is necessary to study the performance of the optimal detector and to compare it with that of mismatch detector. Recall that the structure of the optimal detector is given by (3.20) and Table 3.3 and its performance is shown in Fig. 5.8. We consider the performance under fixed and random timing offset ($T_{il} = T_{ih} = T_i = 0.005$, $i = 1, 2$). As can be seen, the optimal detector outperforms the mismatch detector in high SNR region significantly and the optimal detector will not get worse with the increase of SNR.

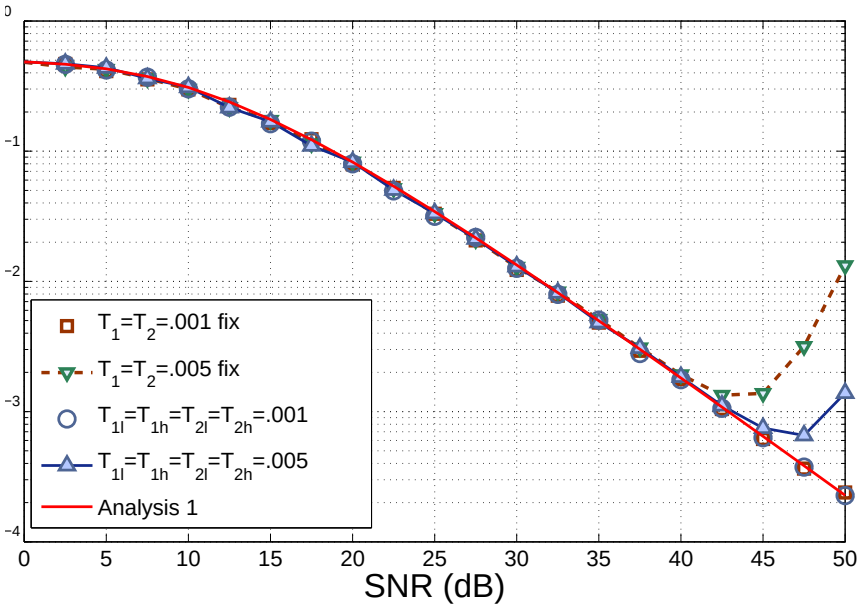

Figure 5.7: Compare the performance of mismatch detector under fixed and random timing offset.

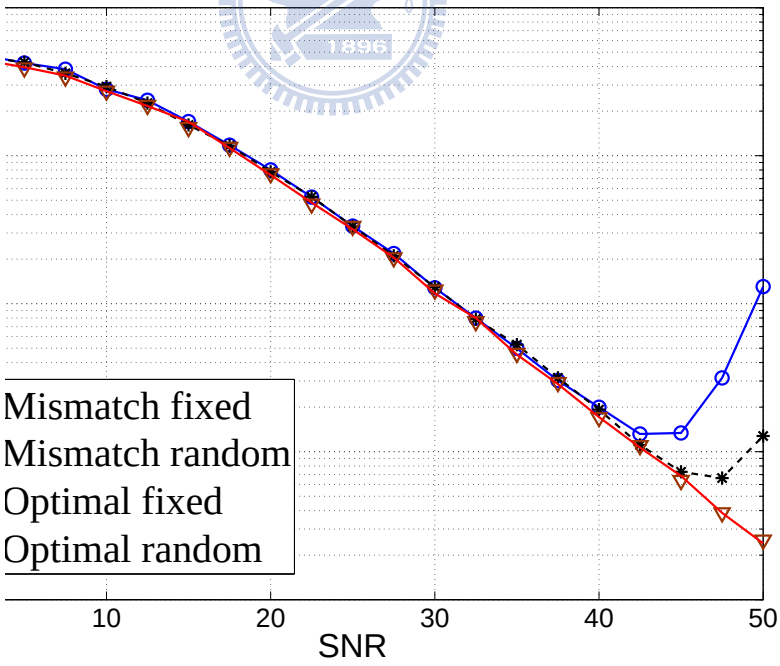

Figure 5.8: Compare the performance of optimal and mismatch detector under fixed and random timing offset ($T_{il} = T_{ih} = T_i = 0.005$, $i = 1, 2$).

Chapter 6

Conclusion and future works

In this thesis, physical layer network coding is considered with BFSK modulation. The optimal detectors with timing alignment error or not is derived through the likelihood ratio test. To make the performance analysis traceable, we propose two suboptimal detectors in the case of perfect timing synchronization. One suboptimal detector is obtained through the max-log approximation and the second one is obtained by further ignoring a term which is very small when SNR is high. Simulation result shows that these two suboptimal detectors have negligible performance loss. Consequentially, it is sufficient to evaluate the performance of these two suboptimal detectors, which is also part of contributions of this thesis. Moreover, we compare the throughput of PNC with that of TPTC and shows that PNC outperforms TPTC in high SNR region (depending on the packet length) in terms of throughput. Finally, we consider the mismatch detector (the optimal detector in the case of perfect timing synchronization) in the presence of timing error. The performance of mismatch detector gets worse with the increase of SNR while it is not true in the case of the optimal detector.

In this thesis, we consider BFSK modulation. To increase data rate, MFSK modulation could be applied. Consequently, the associated optimal detector and performance should be investigated. Moreover, the Rayleigh fading is assumed. In practice, there may exists a direct path between the transmitter and receiver and this results in Rician fading channel. To investigate the Rician fading effect is also one of the future works.

Appendix A

Notations

To describe the structure of PNC we need the following notations.

b_i : the code bit transmitted by node N_i during a particular signaling interval.
$b_i \in \{0, 1\}, \quad i \in \{1, 2\}$.

$x_i(t)$: the baseband signal of node N_i's modulated signal, which is chosen as the b_i^{th} signal of the set of S_F.

$x_{pi}(t)$: bandpass signal which is in connection with $x_i(t)$.

$\mathbf{x}_i$: signal vector with respect to $x_i(t)$, each element shows the bits transmitted by end node N_i.

$y(t)$: the complex envelope of the signal received by the relay node.

$y_p(t)$: the combined bandpass signal received by the relay during one symbol period.

$\mathbf{y}_i$: the output of the BFSK detector placed into the 2×1 complex vector.

h_i : the complex-valued channel gain from node N_i to the relay during signaling interval with the energies of the transmitted signals normalized to unity. $h_i = \alpha_i e^{j\phi_i}$.

α_i : the received amplitude due to the fading.

ϕ_i : the phase shift due to the fading.

$\mathcal{E}_i$: the power of channel gains corresponding to N_i, where $\mathcal{E}_i = E[|h_i|^2] = E[\alpha^2]$.

$n(t)$: additive white Gaussian noise (AWGN) with two-sided noise spectral density N_0.

$\mathbf{n}$: the zero-mean circularly-symmetric complex Gaussian noise with covariance matrix $N_0\mathbf{I}_2$, $\mathbf{I}_2$ is the 2-by-2 identity matrix.

Appendix B

Proofs of lemma 3.2.1, 4.1.2 and 4.1.3

B.1 Proof of lemma 3.2.1

We prove lemma 3.2.1 in this section. This lemma will be used to derive the optimal detector in case 2.

Lemma B.1.1. *Suppose h is $CN(0, \sigma_h^2)$. We have*

$$\int_h \exp\left\{-\frac{|y-h|^2}{N_0}\right\} f(h)dh = \frac{N_0}{N_0+\sigma_h^2} \exp\left\{-\frac{|y|^2}{N_0+\sigma_h^2}\right\} \tag{B.1}$$

Proof. Recall that the pdf of h with variance σ_h^2 is $f(h) = \frac{1}{\pi\sigma_h^2} e^{-\frac{|h|^2}{\sigma_h^2}}$. Then, we have

$$\begin{aligned}
& \int_h \exp\left\{-\frac{|y-h|^2}{N_0}\right\} f(h)dh \\
= & \int_h \exp\left\{-\frac{|y-h|^2}{N_0}\right\} \frac{1}{\pi\sigma_h^2} \exp\left\{-\frac{|h|^2}{\sigma_h^2}\right\} dh \\
= & \frac{1}{\pi\sigma_h^2} \int_h \exp\left\{-\frac{|y-h|^2}{N_0} - \frac{|h|^2}{\sigma_h^2}\right\} dh \\
= & \frac{1}{\pi\sigma_h^2} \exp\left\{-\frac{|y|^2}{N_0+\sigma_h^2}\right\} \int_h \exp\left\{-\frac{N_0+\sigma_h^2}{N_0\sigma_h^2}\left|h - \frac{\sigma_h^2}{N_0+\sigma_h^2}y\right|^2\right\} dh
\end{aligned} \tag{B.2}$$

Since $CN\left(\frac{\sigma_h^2}{N_0+\sigma_h^2}y, \frac{N_0\sigma_h^2}{N_0+\sigma_h^2}\right)$ is a p.d.f, we have

$$\int_h \exp\left\{-\frac{N_0+\sigma_h^2}{N_0\sigma_h^2}\left|h - \frac{\sigma_h^2}{N_0+\sigma_h^2}y\right|^2\right\} dh = \frac{\pi N_0\sigma_h^2}{N_0+\sigma_h^2}.$$

Using this factor, (B.2) becomes

$$\therefore \int_h \exp\left\{-\frac{|y-h|^2}{N_0}\right\} f(h)dh = \frac{1}{\pi\sigma_h^2}\exp\left\{-\frac{|y|^2}{N_0+\sigma_h^2}\right\}\frac{\pi N_0\sigma_h^2}{N_0+\sigma_h^2} = \frac{N_0}{N_0+\sigma_h^2}\exp\left\{-\frac{|y|^2}{N_0+\sigma_h^2}\right\}$$

□

B.2 Proof of lemma 4.1.2

We prove lemma 4.1.2 in this section and, for convenience, lemma 4.1.2 is repeated below.

Lemma B.2.1. *Suppose $x_1 \sim$ exponential(λ_1), $x_2 \sim$ exponential(λ_2) are independent random variables and let $x_M = \max\{x_1, x_2\}$, $x_m = \min\{x_1, x_2\}$. Then, We have*

$$\begin{aligned} f(x_m) &= \frac{\lambda_1+\lambda_2}{\lambda_1\lambda_2}\exp\left\{-\frac{\lambda_1+\lambda_2}{\lambda_1\lambda_2}x_m\right\},\ x_m \geq 0 \\ f(x_M) &= \frac{1}{\lambda_1}\exp\left\{-\frac{x_M}{\lambda_1}\right\} + \frac{1}{\lambda_2}\exp\left\{-\frac{x_M}{\lambda_2}\right\} - \frac{\lambda_1+\lambda_2}{\lambda_1\lambda_2}\exp\left\{-\frac{\lambda_1+\lambda_2}{\lambda_1\lambda_2}x_M\right\},\ x_M \geq 0 \end{aligned}$$

Proof. To find the distribution of x_m, we first calculate the probability of $x_m > x$. Since x_1 and x_2 are independent random variables, we have

$$\begin{aligned} Pr\{x_m > x\} &= Pr\{x_1 > x\}Pr\{x_2 > x\} \\ &= \int_x^\infty \frac{1}{\lambda_1} e^{-\frac{x}{\lambda_1}} dx \int_x^\infty \frac{1}{\lambda_2} e^{\frac{x}{\lambda_2}} dx \\ &= e^{-\frac{\lambda_1+\lambda_2}{\lambda_1\lambda_2}x} \end{aligned}$$

and

$$Pr\{x_m < x\} = 1 - Pr\{x_m < x\} = 1 - e^{-\frac{\lambda_1+\lambda_2}{\lambda_1\lambda_2}x}$$

Hence, the distribution of x_m is

$$f(x_m) = \frac{d\left(Pr\{x_m < x\}\right)}{dx_m} = \frac{\lambda_1+\lambda_2}{\lambda_1\lambda_2} e^{-\frac{\lambda_1+\lambda_2}{\lambda_1\lambda_2}x_m}$$

Similarly, we first calculate the probability of $x_M > x$. Recall that for any two events A, B, we have the equality [16]:

$$Pr(A \cup B) = P(A) + P(B) - P(A \cap B)$$

Using this equality and the fact that x_1 and x_2 are independent, we have

$$\begin{aligned} & Pr\{x_M > x\} \\ = \; & Pr\{x_1 > x\} + Pr\{x_2 > x\} - Pr\{x_1 > x\}Pr\{x_2 > x\} \\ = \; & \int_x^\infty \frac{1}{\lambda_1} e^{-\frac{x}{\lambda_1}} dx + \int_x^\infty \frac{1}{\lambda_2} e^{-\frac{x}{\lambda_2}} dx - \int_x^\infty \frac{1}{\lambda_1} e^{-\frac{x}{\lambda_1}} dx \int_x^\infty \frac{1}{\lambda_2} e^{\frac{x}{\lambda_2}} dx \\ = \; & e^{-\frac{x}{\lambda_1}} + e^{-\frac{x}{\lambda_2}} - e^{-\frac{\lambda_1+\lambda_2}{\lambda_1\lambda_2}x} \end{aligned}$$

and

$$Pr\{x_M < x\} \;\; = \;\; 1 - e^{-\frac{x}{\lambda_1}} - e^{-\frac{x}{\lambda_2}} + e^{-\frac{\lambda_1+\lambda_2}{\lambda_1\lambda_2}x}$$

Take the derivative of the probability, we have the distribution of x_M.

$$f(x_M) = \frac{1}{\lambda_1} e^{-\frac{1}{\lambda_1}x_M} + \frac{1}{\lambda_2} e^{-\frac{1}{\lambda_2}x_M} - \frac{\lambda_1+\lambda_2}{\lambda_1\lambda_2} e^{-\frac{\lambda_1+\lambda_2}{\lambda_1\lambda_2}x_M}$$

□

B.3 Proof of lemma 4.1.3

Lemma B.3.1. *Suppose $x_1 \sim$ exponential(λ_1), $x_2 \sim$ exponential(λ_2). Than the distributions of $z_s = x_1 + x_2$ and $z_d = x_1 - x_2$ are*

$$\begin{aligned} f(z_s) &= \frac{1}{\lambda_2 - \lambda_1}\left(e^{-\frac{z_s}{\lambda_2}} - e^{-\frac{z_s}{\lambda_1}}\right) \\ f(z_d) &= \begin{cases} \frac{1}{\lambda_1+\lambda_2} e^{-\frac{z_d}{\lambda_1}}, & z_d \geq 0 \\ \frac{1}{\lambda_1+\lambda_2} e^{\frac{z_d}{\lambda_2}}, & z_d \leq 0 \end{cases} \end{aligned}$$

Proof. let $z = x_1 + x_2$, then $x_2 = z - x_1$. $I(\cdot)$ means the interval. By the calculation

below, the distribution of z is obtained.

$$\begin{aligned} f(z) &= \int_{-\infty}^{\infty} \frac{1}{\lambda_1} e^{-\frac{x_1}{\lambda_1}} \frac{1}{\lambda_2} e^{-\frac{z-x_1}{\lambda_2}} I(x_1 \geq 0) I(z - x_2 \geq 0)\, dx_1 \\ &= \int_0^z \frac{1}{\lambda_1 \lambda_2} e^{-\left(\frac{1}{\lambda_1} - \frac{1}{\lambda_2}\right) x_1} e^{-\frac{z}{\lambda_2}} dx_1 \\ &= \frac{1}{\lambda_2 - \lambda_1} \left(e^{-\frac{z}{\lambda_2}} - e^{-\frac{z}{\lambda_1}} \right) \end{aligned}$$

Then we will calculate the distribution of $z = x_1 - x_2$. Let $z \leq T$. First we suppose $T \geq 0$, then $x_1 \leq x_2 + T$. From the conditions that x_1, x_2 are under exponential distribution with parameter $lambda_1$, λ_2, we can derive

$$\begin{aligned} Pr\{x_1 - x_2 \leq T\} &= Pr\{x_1 \leq T + x_2\} \\ &= \int_0^{\infty} \int_0^{T+x_2} \frac{1}{\lambda_1} e^{\frac{x_1}{\lambda_1}} \frac{1}{\lambda_2} e^{-\frac{x_2}{\lambda_2}} dx_1 dx_2 = 1 - \frac{\lambda_1}{\lambda_1 + \lambda_2} e^{-\frac{T}{\lambda_1}} \end{aligned}$$

after differential we have

$$f(x_1 - x_2) = \frac{1}{\lambda_1 + \lambda_2} e^{-\frac{T}{\lambda_1}}$$

Then we suppose $T \leq 0$, where $x_1 - T \leq x_2$. By the operation similar as before,

$$\begin{aligned} Pr\{x_1 - x_2 \leq T\} &= Pr\{x_1 - T \leq x_2\} \\ &= \int_0^{\infty} \int_{x_1 - T}^{\infty} \frac{1}{\lambda_1} e^{\frac{x_1}{\lambda_1}} \frac{1}{\lambda_2} e^{-\frac{x_2}{\lambda_2}} dx_2 dx_1 = \frac{\lambda_2}{\lambda_1 + \lambda_2} e^{\frac{T}{\lambda_2}} \end{aligned}$$

then,

$$f(x_1 - x_2) = \frac{1}{\lambda_1 + \lambda_2} e^{\frac{T}{\lambda_2}}$$

□

Bibliography

[1] Y. Wu, P. A. Chou, S. -Y. Kung, "Information Exchange in Wireless Networks with Network Coding and Physical-layer Broadcast," in *Proc., Conf. Inform. Sci. and Systems (CISS),* Baltimore, MD, Mar. 2005.

[2] J. Crowcroft, S. Katti, H. Rahul, W. Hu, D. Katabi, M. Médard, "XORs in the Air: Practical Wireless network Coding," in *IEEE/ACM Trans. Netw.,* pp. 497-510, June. 2008.

[3] S. Zhang, S. C. Liew, and P. P. Lam, "Physical-Layer Network Coding," in *Proc. MobiComm,* pp. 358-365, 2006.

[4] S. Zhang, S. C. Liew, "Applying Physicl-Layer Network Coding in Wireless Networks," *EURASIP Journal on Wireless Commun. and Netw.,* vol. 2010, Article ID 870268, 12 pages, 2010. doi:10.1155/2010/870268

[5] R. -H. Y. Louie, Y. Li, B Vucetic, "Practical PhysicalLayer Network Coding for Two-Way Relay Channels: Performance Analysis and Comparison," in*IEEE Trans. Wireless Commun.,* vol. 9, no 2, Feb. 2010.

[6] K. Lu, S. Fu, Y. Qian, H. -H. Chen, "SER Performance Analysis for Physical Layer Network Coding over AWGN Channels," in *GLOBECOM 2009. IEEE.,* pp. 1-6, Nov. 2009.

[7] D. To, J. Choi, I. -M. Kim, "Error Probability Analysis of Bidirectional Relay Systems Using Alamouti Scheme," in *Commun. Letters, IEEE,* pp. 758-760, Nov. 2010.

[8] S. Zhang, S. -C. Liew, P P. LAM, "On the Synchronization of Physical-Layer Network Coding," in *Inf. Theory Workshop,* pp. 404-408, Oct. 2006.

[9] M. C. Valenti, D. Torrieri, and T. Ferrett, "Noncoherent physical-layer network coding using binary CPFSK modulation," in *Proc. IEEE Military Commun. Conf.,* pp. 1-7, Oct. 2009.

[10] J. H. Sorensen, R. Krigslund, P. Popovski, T. K. Akino, and T. Larsen, "Physical-Layer Network Coding for FSK System," in *IEEE Commun. Lett,* pp. 597-599, Aug. 2009.

[11] Y. T. Su, Y. S. Shen, and C. Y. Hsiao, "On the Detection of a Class of Fast Frequency-Hopped Multiple Access Signals," in *IEEE J. Sel. Areas Commun.,* vol. 19, no. 11, pp.2151-2164, Nov. 2001.

[12] S. Hinedi, M. Simon, and D. Raphaeli, "The Performance of Noncoherent Orthogonal M-FSK in the Presence of Timing and Frequency Errors," in *IEEE Trans. Commun.,* vol. 43, pp. 922-933, Feb/Mar/Apr 1995.

[13] J. L. Massey, "Optimum Frame Synchronization," in *IEEE Trans. Commun. ,* pp. 115-119 Apr 1972.

[14] H. L. Van Trees, "Detection, estimation, and modulation theory. Part I: Detection, estimation, and linear modulation theory," John Wiley & Sons, Inc., 2001.

[15] P. Robertson, E. Villebrun, and P. Hoeher, "A comparison of optimal and sub-optimal MAP decoding algorithms operating in the log domain," in *Proc. IEEE Int. Conf. Commun.*, Seattle, Washington, pp. 1009-1013, Jun. 1995.

[16] G. Casella, R.L. Berger, *Statistical Inference,* Duxbury Press, 2 ed., 2001.